JOURNAL OF THE ROYAL SOCIETY Interface

rsif.royalsocietypublishing.org

Headline review

Biological energy conversion

Cite this article: Barber J, Tran PD. 2013 From natural to artificial photosynthesis. J R Soc Interface 10: 20120984. http://dx.doi.org/10.1098/rsif.2012.0984

Received: 28 November 2012
Accepted: 9 January 2013

Subject Areas:
bioengineering

Keywords:
artificial leaf, hydrogenases, photosystem II, solar energy, solar fuels, water splitting

Author for correspondence:
James Barber
e-mail: j.barber@imperial.ac.uk

From natural to artificial photosynthesis

James Barber[1,2,3] and Phong D. Tran[2,4]

[1]Division of Molecular Biosciences, Department of Life Sciences, Imperial College London, London, UK
[2]Solar Fuel Laboratory, School of Materials Science and Engineering, Nanyang Technological University, Singapore
[3]BioSolar Laboratory, Applied Science and Technology Department, Politecnico di Torino, Viale T. Michel 5, 15121 Alessandria, Italy
[4]Energy Research Institute, Nanyang Technological University, Singapore

Demand for energy is projected to increase at least twofold by mid-century relative to the present global consumption because of predicted population and economic growth. This demand could be met, in principle, from fossil energy resources, particularly coal. However, the cumulative nature of carbon dioxide (CO_2) emissions demands that stabilizing the atmospheric CO_2 levels to just twice their pre-anthropogenic values by mid-century will be extremely challenging, requiring invention, development and deployment of schemes for carbon-neutral energy production on a scale commensurate with, or larger than, the entire present-day energy supply from all sources combined. Among renewable and exploitable energy resources, nuclear fusion energy or solar energy are by far the largest. However, in both cases, technological breakthroughs are required with nuclear fusion being very difficult, if not impossible on the scale required. On the other hand, 1 h of sunlight falling on our planet is equivalent to all the energy consumed by humans in an entire year. If solar energy is to be a major primary energy source, then it must be stored and despatched on demand to the end user. An especially attractive approach is to store solar energy in the form of chemical bonds as occurs in natural photosynthesis. However, a technology is needed which has a year-round average conversion efficiency significantly higher than currently available by natural photosynthesis so as to reduce land-area requirements and to be independent of food production. Therefore, the scientific challenge is to construct an 'artificial leaf' able to efficiently capture and convert solar energy and then store it in the form of chemical bonds of a high-energy density fuel such as hydrogen while at the same time producing oxygen from water. Realistically, the efficiency target for such a technology must be 10 per cent or better. Here, we review the molecular details of the energy capturing reactions of natural photosynthesis, particularly the water-splitting reaction of photosystem II and the hydrogen-generating reaction of hydrogenases. We then follow on to describe how these two reactions are being mimicked in physico-chemical-based catalytic or electrocatalytic systems with the challenge of creating a large-scale robust and efficient artificial leaf technology.

1. Introduction

Natural photosynthesis is the process by which sunlight is captured and converted into the energy of chemical bonds of organic molecules that are the building blocks of all living organisms and also of oil, gas and coal. These fossil fuels are the products of photosynthetic activity millions of years ago and provide us with most of the energy needed to power our technologies, heat our homes and produce the wide range of chemicals and materials that support everyday life. Sooner or later, the readily available reserves of fossil fuels will become scarce and then what? Even before then, as a consequence of our ever-growing use of oil, gas and coal, we are faced with the problem of increasing levels of CO_2 and other greenhouse gases in the atmosphere with implications for global climate change.

Royal Society Publishing
Informing the science of the future

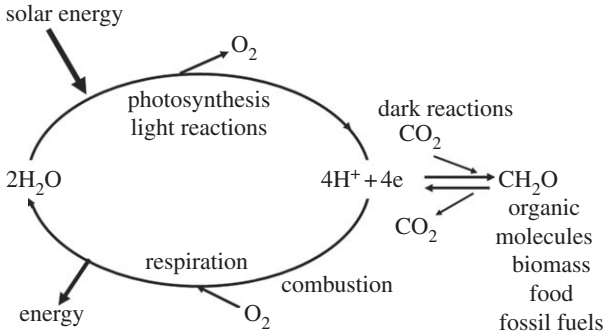

Figure 1. A diagrammatic representation of energy flow in biology. The light reactions of photosynthesis (light absorption, charge separation, water splitting, electron/proton transfer) provides the reducing equivalents in the form of energized electrons (e) and protons (H^+) to convert carbon dioxide (CO_2) into carbohydrates (CH_2O) and other organic molecules which make up living organisms (biomass), including those that provide humankind with food. The same photosynthetic reactions gave rise to the fossil fuels formed millions of years ago. The burning of these organic molecules either by respiration (controlled oxidation within our bodies) or by combustion of biomass and fossil fuels to power our technologies, is the reverse to photosynthesis, releasing CO_2 and combining the stored 'hydrogen' back with oxygen to form water. In so doing energy, which is originated from sunlight, is released.

The success of photosynthesis as an energy-generating and -storage system stems from the fact that the raw materials and power needed for the synthesis of biomass are available in almost unlimited amounts; sunlight, water and CO_2. At the heart of the photosynthetic process is the splitting of water by sunlight into oxygen and hydrogen equivalents. The oxygen is released into the atmosphere where it is available for living organisms to breathe and for burning fuels to drive our technologies. The hydrogen equivalents are used to reduce CO_2 to sugars and other organic molecules of various types. When we burn fuels (fossil, biomass and other biofuels) to release energy, we are simply combining the 'hydrogen' stored in these organic molecules with atmospheric oxygen to form water, so completing a cycle started millions of years ago. Similarly, energy is also released from the organic molecules which constitute our food, when they are metabolized within our bodies by the process of respiration. Thus, in the biological world, photosynthesis brings about the splitting of water into oxygen and 'hydrogen', whereas respiration is the reverse, combining oxygen and hydrogen in a carefully controlled and highly efficient way so as to create metabolic energy. Therefore, from an energetic view, the synthesis of organic molecules represents a way of storing hydrogen and therefore storing solar energy in the form of chemical bonds (figure 1).

In this study, we will briefly emphasize the enormity of the energy/CO_2 problem that we face within the coming decades and discuss the contributions that could be made by fuels derived directly from developing new technologies based on the successful principles of natural photosynthesis. We will particularly emphasize the possibility of exploiting the vast amounts of solar energy available to split water to produce dioxygen and the hydrogen equivalents required to produce fuels such as alcohols and methane, and particularly the simplest of all solar fuels, hydrogen gas. This technology we will refer to as artificial photosynthesis.

2. Global energy consumption and the enormity of the problem

At the present time, the rate of global energy consumption is in the region of 16.3 TW [1], with the USA and the extended EU each representing about 40 per cent of this. In future, this global value will rise owing to industrialization in underdeveloped and developing countries coupled with increasing world population. Based on current projections, the global annual energy consumption rate will reach 20 TW or more by 2030, doubled by 2050 and tripled by the end of the century [2–4]. About 85 per cent of the total global energy consumed at present comes from burning fossil fuels with the proportion approaching 90 per cent for developed countries. Oil, gas and coal contribute approximately equally to this demand. The remaining sources of energy are hydroelectric, nuclear, biomass and renewable, such as solar, wind, tide and wave. At present, the use of biomass is a major player and is mainly localized in underdeveloped regions such as Africa and India where wood and other organic matter is used as a fuel. Much of this is not strictly renewable, because there is no planned regeneration and the trend is towards more use of fossil fuels.

The low level of contribution of non-fossil energy sources to present-day global energy demand reflects the readily available resources of oil, gas and coal. Even when oil reserves become limiting, there will remain large reservoirs of gas (including from shale) and, particularly, coal to exploit [5]. Therefore, in the global arena, the problem for the immediate future is not a limitation of fossil fuel reserves but the consequences of its combustion. If the total fossil fuel reserve is burnt, then the CO_2 level in the atmosphere and oceans would rise to values equivalent to those that existed on our planet long before humankind evolved [6]. Despite this consideration, it is certain that fossil fuels will continue to be a major source of energy for humankind for some years to come but it is vital that they should be used in such a way as to minimize CO_2 release into the atmosphere. Technologies for sequestration of CO_2 must be developed [7]. Hand in hand with this, there will almost certainly be an improvement in the efficiency of energy use and supplementation whenever possible from non-fossil fuel sources. Against this background, we must also strive to develop new technologies based on principles that have yet to be revealed from basic studies and in particular those that focus on using the enormous amount of energy available to us as solar radiation [8]. The sun provides solar energy to our planet on an annual basis at a rate of 100 000 TW. Therefore, the energy from 1 h of sunlight is equivalent to all the energy humankind currently uses in a year. We do have existing technologies to capture sunlight and produce electricity and the efficiency and robustness of these photovoltaic systems is improving daily [9,10]. Compared with the present-day price of fossil fuels, photovoltaic systems represent an expensive way to generate electricity because of the high cost of their construction. In time, these costs will decrease relative to the cost of fossil fuel. Moreover, a blending of the principles of photovoltaic systems, especially those using cheap organic or inorganic materials, with concepts

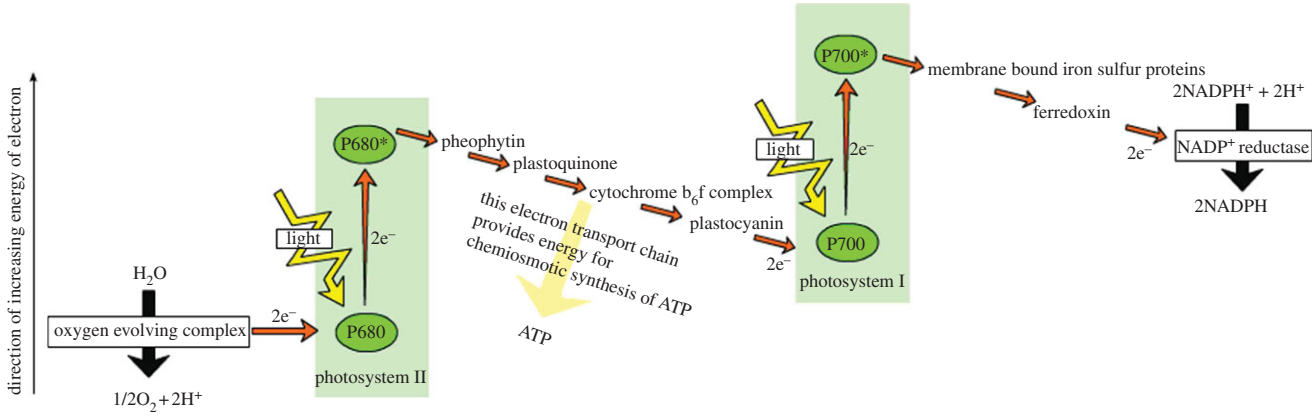

Figure 2. A simplified Z-scheme of the light reactions of photosynthesis taken from http://en.wikipedia.org/wiki/photosynthesis. For every electron extracted from water and transferred to CO_2, the energy of two photons of light is required. One is absorbed by photosystem II (PSII) that generates a strong oxidizing species ($P680^+$), able to drive the water-splitting reaction and a reduction of pheophytin (Pheo) and then plastoquionel (Q) to plastoquinol (QH_2). The other photosystem, photosystem I (PSI) generates a strong reducing species, NADPH, which donates reducing equivalents to CO_2 to produce sugars and other organic molecules, and a weak oxidant $P700^+$. Electron and proton flow from QH_2 to $P700^+$ is aided by the cytochrome b_6f (Cyt b_6f) complex and plastocyanin (PC) and results in the release of energy to convert ADP to ATP. The ATP produced is required, along with NADPH, to convert CO_2 to sugars. Because the production of O_2 requires the splitting of two water molecules, the overall process involves the removal of two electrons per water molecule as shown and therefore four photons per PSII and PSI reaction centre. The reduction of oxidized nicotinamide adenine dinucleotide phosphate ($NADP^+$) by PSI is facilitated by membrane bound iron sulfur proteins (F_X, F_A and F_B) and soluble ferredoxin (F_D).

derived from natural photosynthetic systems may ultimately provide a long-term solution in the form of artificial photosynthesis technology [4,8]. In considering this long-term solution, let us take a look at the efficiency of the natural photosynthetic process.

3. Natural photosynthesis

3.1. Efficiency

As emphasized in figure 1, photosynthesis is a process that converts light energy into the organic molecules of biomass which is composed of mainly carbohydrates symbolized as CH_2O. To estimate the efficiency of this process, two main factors must be appreciated.

(i) Although photosynthetic organisms can efficiently trap light energy at all wavelengths of visible solar radiation, the energy used for splitting water and reducing CO_2 is only equivalent to the red region of the spectrum. Higher energy photons are degraded to heat by internal conversion within the light-harvesting pigments to the energy level of 'red' photons at about 1.8 eV.

(ii) For every electron/proton extracted from water and used to reduce CO_2, the energy of two 'red' photons is required. This is accomplished by linking together, in series, two different photosystems, photosystem II (PSII), which uses light to power the extraction of electrons/protons from water, and photosystem I (PSI), which uses light to provide additional energy to the 'PSII-energized' electrons/protons so as to drive the CO_2-fixation process (figure 2). Therefore, in photosynthesis, the energy of at least eight 'red' photons is required per O_2 molecule released or CO_2 molecule fixed. A typical product of carbon fixation is glucose ($C_6H_{12}O_6$) whose energy content is 673 kcal per quantum mole (2805 kJ $mole^{-1}$) when burnt in a calorimeter. To make a glucose molecule, the energy of 48 'red' photons is required and assuming a wavelength of 680 nm, corresponding to 42 kcal per quantum mole (175 kJ $mole^{-1}$), gives the efficiency of conversion at about 30 per cent. Although this is an impressive number, in reality, the overall conversion of solar energy to the glucose and the very large variety of other organic molecules that constitutes biomass, is much lower. Energy is lost through degrading shorter wavelength light (e.g. blue light) to the energy of 'red' photons, by saturation processes and more significantly, in driving the enormous number of reactions that occur in photosynthetic organisms to maintain their organization, metabolism, reproduction and survival. Taking these various factors into account, the estimated maximum efficiency of photosynthesis is about 4.5 per cent [11–15].

In fact, an efficiency of 4.5 per cent is rarely reached. Only in exceptional cases will dry matter yield exceed 1 or 2 per cent, such as with the intense growing of sugar cane in tropical climates or with optimized culturing of algae. Normally, agricultural crops produce yields of biomass at efficiencies less than 1 per cent, even when pampered with ample supplies of fertilizer and water. Environmental conditions, degree of light interception, nutrient and water supply are key factors in reducing the efficiency below the maximum, whereas specific genetic characteristics of particular plant species also dictate growth rates and maximum yields of biomass.

On a global basis, the efficiency of photosynthesis is significantly lower than for agricultural and energy crops or algal cultures growing under optimal conditions because of seasonal changes and the existence of large portions of land and oceans on our planet that do not sustain significant levels of photosynthetic activity [13]. Thus, the rate of energy storage averaged over a year by photosynthesis is 100 TW, representing just 0.1 per cent conversion given that solar energy arriving at our planet is at a rate of 100 000 TW over the same time period. This energy is mainly stored in wood and fibres of terrestrial trees and plants. A similar amount of photosynthetic activity occurs in the oceans, but there the fixed carbon is rapidly recycled into the food chain [16]. Therefore, an approximate efficiency of global photosynthesis is 0.2 per cent but with only half

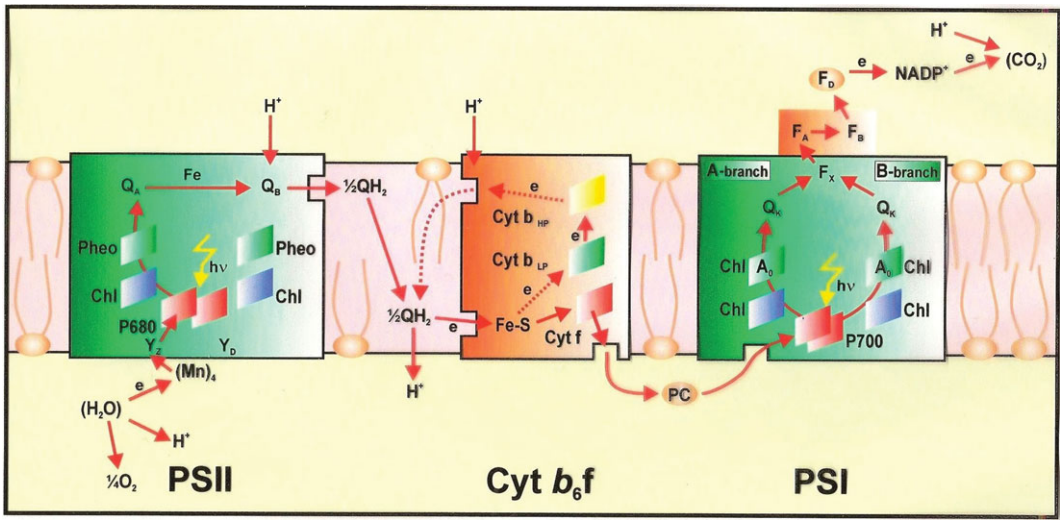

Figure 3. Schematic of the electron–proton transport chain of oxygenic photosynthesis in the thylakoid membrane, showing how photosystem I (PSI) and photosystem II (PSII) work together to use absorbed light to oxidize water and reduce $NADP^+$, in an alternative representation to the Z-scheme shown in figure 2. The diagram also shows how the vectorial flow of electrons across the membrane generates a proton gradient which is used to power the conversion of ADP to ATP at the ATP synthase complex (CF_0CF_1) which is also embedded in the thylakoid membrane (not shown). In both PSI and PSII, the redox-active cofactors are arranged around a pseudo-twofold axis. In PSII, primary charge separation and subsequent electron flow occurs along one branch of the reaction centre. However, in the case of PSI, electron flow occurs up both branches as shown. Electron flow through the cytochrome b_6f complex also involves a cyclic process known as the Q cycle. Y_Z = tyrosine; P680 = primary electron donor of PSII composed of chlorophyll (Chl); Pheo = pheophytin; Q_A and Q_B = plastoquinone; Cyt b_6f = cytochrome b_6f complex, consisting of an Fe–S Rieske centre, cytochrome f (Cyt f), cytochrome b low- and high-potential forms (Cyt b_{LP} and Cyt b_{HP}), plastoquinone binding sites, Q_1 and Q_0; PC = plastocyanin; P700 = primary electron Chl donor of PSI; A_0 = Chl; A_1[Q] = phylloquinone; F_X, F_A and F_B = Fe–S centres, F_D = ferredoxin; FNR = ferredoxin NADP reductase; $NADP^+$ = oxidized nicotinamide adenine dinucleotide phosphate. Y_D = symmetrically related tyrosine to Y_z but not directly involved in water oxidation, and QH_2 = reduced plastoquinone (plastoquinol), which acts as a mobile electron/proton carrier from PSII to the cytochrome b_6f complex. With the exception of the mobile electron carriers Q/QH_2, PC and F_D, the remaining redox-active cofactors are bound to multisubunit protein complexes that span the membrane depicted as coloured boxes.

being stored in biomass. Of course, it was terrestrial biomass that was the major source of energy for humankind prior to the exploitation of fossil fuels. It is not surprising, therefore, that there is now a growing interest in returning to the use of biomass and biofuels as an alternative to fossil fuels, because their production and use is CO_2 neutral. However, the scale required for satisfying the current global energy requirement is far from attainable because of competing with large-scale food production and general land use needs to sustain a global population of seven billion.

Although it may be possible to engineer plants and other types of photosynthetic organisms (algae) as energy-converting 'machines' and 'chemical factories', the overall efficiency of solar energy conversion will rarely exceed 1 per cent and will usually be much less, so much so that this approach can make only a minor contribution to our future energy requirements. However, the efficiencies of the early photochemical and chemical reactions of photosynthesis, which are not directly involved in biomass production, are significantly higher. Because of this, there are alternative and complementary approaches for using solar energy. For example, it may be possible to develop a highly efficient, artificial, molecular-based, solar-energy-converting technology that exploits the principles of the 'front-end' of natural photosynthesis. Indeed, our knowledge of the natural process is such as to provide a blueprint for the design and assembly of such 'artificial photosynthetic' devices as described in the following sections.

3.2. Molecular processes

As emphasized earlier, photosynthesis has produced most of the energy that fuels human society and sustains life on our planet. The process is underpinned by the light-driven water-splitting reaction that occurs in PSII of plants, algae and cyanobacteria (figure 2). Solar energy is absorbed by chlorophyll and other pigments, and is transferred efficiently to the PSII reaction centre where charge separation takes place. This initial conversion of light energy into electrochemical potential occurs in the reaction centre of PSII with a maximum thermodynamic efficiency of about 70 per cent and generates a radical pair state $P680^{\bullet+}Pheo^{\bullet-}$, where P680 is a chlorophyll *a* molecule, and Pheo is a pheophytin *a* molecule (chlorophyll molecule without a Mg ion ligated into its tetrapyrrole head group). The redox potential of $P680^{\bullet+}$ is highly oxidizing, estimated to be about +1.2 V, while that of $Pheo^{\bullet-}$ is about −0.5 V. The latter is sufficiently negative such that, in principle, it could drive the formation of hydrogen. Instead, the reducing equivalent is passed along an electron transport chain to PSI (figure 2), where it is excited by the energy of a second 'red' photon absorbed by a chlorophyll molecule, known as P700, to lift it to a reducing potential of −1 V or more. In this way, sufficient energy is accumulated to drive the fixation of CO_2, which not only requires the generation of the reduced 'hydrogen carrier', nicotinamide adenine dinucleotide phosphate (NADPH), but also the energy-rich molecule adenosine triphosphate (ATP) formed by the release of some energy during electron transfer from PSII to PSI (in the form of an electrochemical potential gradient of protons; figures 2 and 3). The $P680^{\bullet+}$ species generated in PSII drives the splitting of water at the 'water oxidizing centre' (WOC). It does so by extracting electrons from a catalytic centre composed of a cluster of four manganese (Mn) ions and a calcium ion (Ca^{2+}). The splitting of water into dioxygen and reducing equivalents is a

four-electron process and therefore PSII must absorb four photons (4 hν) to drive this half-reaction with PSI also using 4 hν to give sufficient potential for subsequent reductive reactions. $2H_2O + 4h\nu \rightarrow O_2 + 4H^+ + 4e^-$.

The reducing equivalents leave PSII in the form of plastoquinol (QH_2), whereas the dioxygen is released into the atmosphere. $4H^+ + 4e^- + 2Q \rightarrow 2QH_2$.

The efficiency of this reaction is high being almost 55 per cent when driven by the energy of 'red' photons but decreases to about 20 per cent when taking into account the fact that light is absorbed across the whole solar spectrum. Of course, in photosynthetic organisms, the reaction can proceed only continuously when the QH_2 molecules are oxidized by the light absorbed by PSI, thus allowing reducing equivalents to be transferred to $NADH^+$ and then to CO_2. Because of this saturation effect, the quantum efficiency of photosynthetic water splitting is further decreased.

The light-driven transfer of electrons and protons from H_2O to CO_2 involves a number of redox-active cofactors located in the PSII and PSI protein complexes (see figure 3 and its legend for specific details). The transfer of reducing equivalents between PSII and PSI is aided by a third membrane protein complex known as cytochrome b_6f (Cyt b_6f) as detailed in figure 3. The three complexes, PSI, PSII and Cyt b_6f, are located in the photosynthetic membrane such that electron flow from water to $NADP^+$ is vectorial, leading to the generation of a proton gradient across the membrane (figure 3). This gradient is used chemiosmotically by a fourth complex, CF_0–CF_1, to drive its ATP synthase activity to convert ADP to ATP and thus provide chemical energy for the CO_2-reduction process (for details, see reference [17]).

In many ways, the photosystems of photosynthesis, including those of anoxygenic photosynthetic bacteria (organisms that do not split water) are highly efficient molecular photovoltaic nanomachines in that they use light energy to bring about electrical charge separation across a membrane of high dielectric strength [18]. The organization of the electron carriers and other cofactors in these nanomolecular devices are optimized to facilitate forward energy-storing reactions and minimizing backward and wasteful-energy-releasing reactions. There is considerable information about these photosystems which indicates that they are structurally and functionally very similar [19,20]. Indeed, there are aspects of their design that provide a blue print for constructing 'artificial photosynthetic' systems.

Similarly, the light-harvesting systems associated with the photosystems of different types of photosynthetic organisms have common principles for capturing solar energy across the whole of the visible spectrum and facilitating efficient energy transfer to the associated reaction centres with minimum loss of energy. Again, detailed spectroscopic and structural studies have revealed the molecular basis of these systems, details that could also be adopted for designing light-concentrating systems for a new generation of solar-energy-converting technologies [21].

However, it is the water-splitting reaction of PSII that holds the greatest promise for the development new technologies for converting solar radiation into usable energy, particularly, in generating hydrogen equivalents for reducing CO_2. In this way, PSII is unique when compared with all other types of photosystems that are far more limited in the redox chemistry they catalyse.

3.3. Photosystem II

The photosynthetic water-splitting reaction appeared on our planet about 2.5 billion years ago and was the 'big bang of evolution' since for the first time living organisms had available an inexhaustible supply of 'hydrogen' (in the form of hydrogen equivalents) to convert CO_2 into organic molecules. From that moment, living organisms on the Earth could prosper and diversify on an enormous scale; biology had solved its energy problem and PSII established itself as the 'engine of life' [22].

Clearly, using solar energy to split water to produce hydrogen equivalents or 'high energy' electrons is also the perfect solution for humankind. In principle, the technology exists today to do this. Electricity can be generated by photovoltaic solar cells and used to carry out the electrolysis of water. With a solar cell efficiency of 10 per cent and 65 per cent efficiency for the electrolytic system, the overall efficiency would be 6.5 per cent. Electrolysis relies on platinum or other catalysts for gas evolution, which are in limiting supply and therefore expensive. At present very little hydrogen is produced by electrolysis because it is more economical to generate from fossil fuels. Similarly, the cost of photovoltaic solar cells marginalizes this route for using solar energy to produce hydrogen directly from water. The challenge is to devise a water-splitting catalyst that is robust and composed of abundant non-toxic materials that work along similar chemical principles to those used by the WOC of PSII.

Because of the importance of understanding the chemistry of the water-splitting reaction of PSII, there has been a wide range of techniques applied to probe the molecular mechanisms involved and to investigate the structure of the catalytic centre (see various articles in references [23,24]), being particularly spurred by the recent structural analyses of PSII by X-ray absorption spectroscopy [25–27] and X-ray crystallography [28–32]. These studies, coupled with quantum mechanical analyses, have provided a refinement of the structure of the WOC [33–35] and given detailed schemes for the water-splitting chemistry leading to O–O bond formation [36–43].

It is now clear that the water-splitting reaction takes place at a catalytic centre consisting of three Mn ions and a Ca ion forming a cubane-like structure with the four metal ions linked by oxo-bridges. A fourth Mn ion is linked to the cubane by two oxo-bridges and is adjacent to the Ca ion. This general arrangement was first suggested by Ferreira *et al.* [30] and recently confirmed, refined and improved in a 1.9 Å X-ray derived model [32] (figure 4*a*). Surrounding the Mn_4Ca-cluster are a number of amino acid residues that either provide ligands to the metal ions or act to facilitate hydrogen bonding networks that almost certainly play a key role in the deprotonation of the substrate water molecules (figure 4*b*).

With structural information available, realistic chemical schemes are now being formulated for the water-splitting reaction and the formation of molecular oxygen. It has been known, for some time, that there are at least five intermediate states leading to the formation of dioxygen, known as S-states [44].

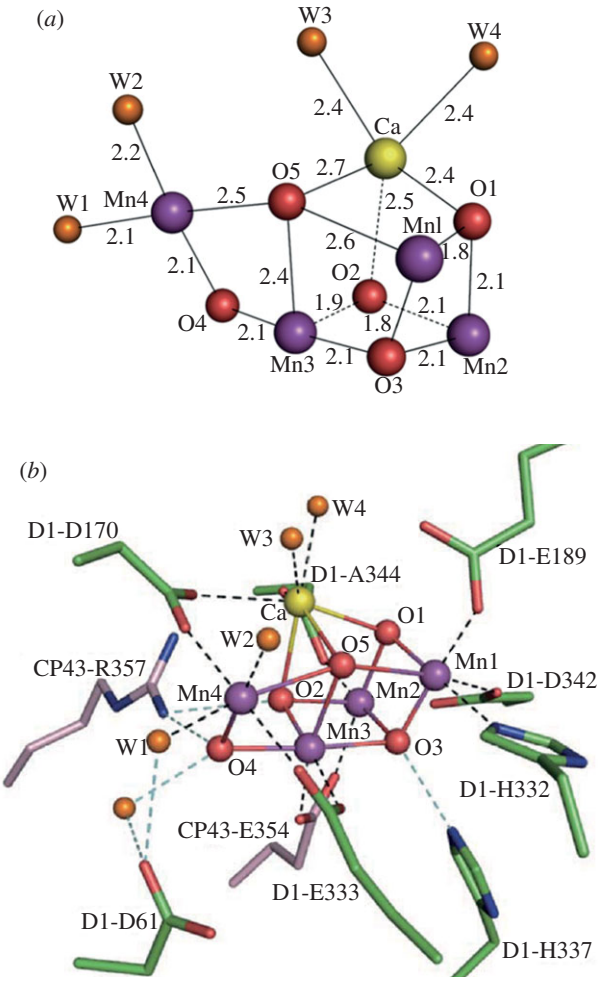

Figure 4. (*a*) Structure of the Mn_4CaO_5 cluster and (*b*) its ligand environment as determined at a resolution of 1.9 Å by Umena *et al.* [32].

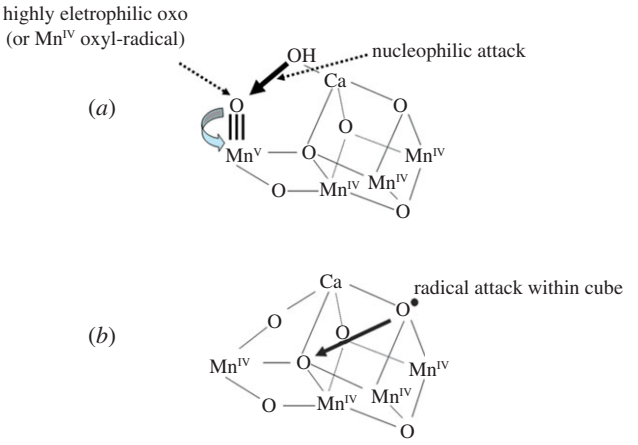

Figure 5. Two different mechanisms for the final step of the S-state cycle when the dioxygen bond of O_2 is formed. (*a*) Mechanism 1. The very high oxidation state of the Mn-cluster, particularly the Mn ion outside the Mn_3CaO_4-cubane, leads to a high electron deficient oxo (after deprotonation of water molecules during the S-state cycle). Nucleophilic attack by the hydroxide of the second substrate water within the coordination sphere of Ca^{2+} leads to O_2 formation. (*b*) Mechanism 2. The formation of an oxo-radical within the Mn_3CaO_4-cubane attacks a bridging oxo species to form the O–O bond. (Online version in colour.)

The sequential advancement from S_0 to S_4 is driven by each photochemical turnover. The progression through the S-states to S_4 results in the storing of four oxidizing equivalents, which are reduced in the final step (S_4–S_0) by four electrons derived from two substrate water molecules with the concomitant formation of dioxygen.

Although the geometry of the Mn_4Ca-cluster and its exact ligand field characteristics are now known at a high resolution, there has been concern that it represents a more reduced form of the cluster than that of S_0 because free electrons are generated during the collection of the X-ray diffraction data. This concern has been countered by recent studies [45–48]. Despite some uncertainties about the exact S-state represented by the high-resolution model, it is providing a basis for developing chemical mechanisms for the water oxidation and dioxygen formation. The Mn ion linked to the cubane structure (Mn_4) is immediately adjacent to the Ca^{2+} and their positioning towards the side chains of several key amino acids, including the redox-active Y_Z, suggests that they provide the 'catalytic' surface for binding the substrate water molecules and their subsequent oxidation. Indeed, the 1.9 Å structure has revealed two water molecules bound to each of the ions. In fact, they are the only water molecules directly ligated to the metal cluster. One well-championed mechanism suggests that the substrate water, associated with Mn_4, is deprotonated during the S-state cycle and converted into a highly electrophilic oxo (figure 5*a*) [36–40]. This mechanism is dependent on Mn_4 being converted to a high oxidation state (possible Mn(V)) during progression to the S_4-state just prior to O–O bond formation. The other three Mn ions are progressively driven into high valency states (Mn(IV)) and act as a further 'oxidizing battery' for the Mn(V)-oxo species in the S_4-state. In this way, the reactive oxo is electron deficient, so much so that it makes an ideal target for a nucleophilic attack by the oxygen of the second substrate water bound within the coordination sphere of the Ca^{2+} (figure 5*a*).

An alternative mechanism proposed by Siegbahn, which is based on in depth DFT calculations, suggests that an oxo-radical forms within the Mn_3CaO_4-cubane and attacks a bridging oxo species to form the O–O bond (figure 5*b*) [41–43]. The DFT calculations did not support the alternative mechanism shown in figure 5*a*, and experimental support has recently emerged in favour of the Siegbahn mechanism [49,50].

3.4. Hydrogenases

Many microorganisms, including some which have photosynthetic activity, have the ability to either extract electrons from hydrogen molecules to power their metabolism or remove excess low-potential electrons by reducing protons and releasing hydrogen. This microbial inter-conversion between hydrogen consumption and release is efficiently mediated by metalloenzymes, named hydrogenases. These hydrogenases are divided into two main classes: [NiFe]- and [FeFe]-hydrogenases, based on the chemical composition of their catalytic sites [51–53]. A third class, [Fe]-hydrogenases, catalyses the reversible reduction of methenyltetrahydromethanopterin with hydrogen to methylenetetrahydromethanopterin and protons [54].

The catalytic active sites of the [NiFe]- and [FeFe]-hydrogenases consist of a bimetallic centre whose coordination is provided by residual cysteine, dithiolate and surprisingly, CO and CN^- ligands where the latter pair are unusual in biology

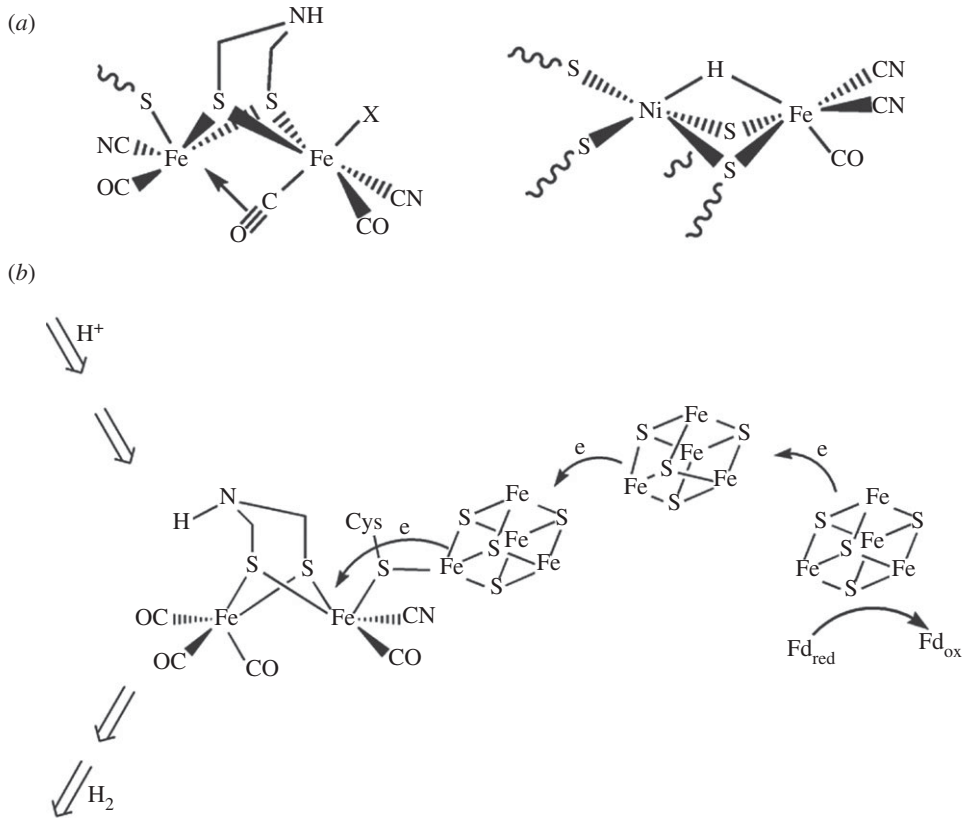

Figure 6. Catalytic active sites of [FeFe]- and [NiFe]-hydrogenases (*a*); schematized structure and function of [FeFe]-hydrogenase for hydrogen evolution reaction (*b*). Schematized electron, proton and hydrogen transfer pathways are included.

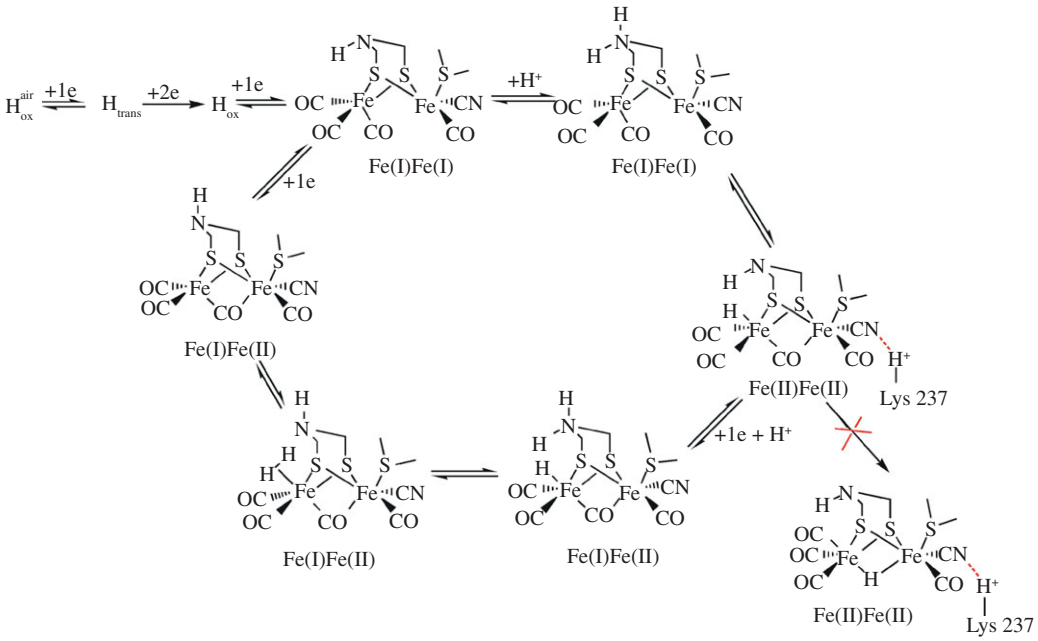

Figure 7. Proposed activation of [FeFe]-hydrogenase and catalytic cycle for hydrogen evolution reaction [57–59].

(figure 6*a*) [51–53]. These active sites are buried within the specific protein environments that function to tune the catalytic activity. The transfer of protons and molecular hydrogen is facilitated by a specific proton transfer pathway and by gas channels, whereas the [FeS] clusters ensure the transfer of electrons between ferredoxin, the redox mediator bound to the protein surface and the catalytic site (figure 6*b*) [55]. As shown by electrochemical studies, hydrogenases are as electrocatalytically active as platinum nanoparticles are for hydrogen evolution and uptake [56].

A simplified mechanism for the proton-reduction reaction in [FeFe]-hydrogenase is given in figure 7 [57–59]. The first step is thought to be the protonation of the azapropanedithiolate ligand that lowers the redox potential of the catalytic centre, commonly referred to as H-cluster. Reduction of this protonated system results in the formation of a highly active terminal hydride that rapidly generates hydrogen gas via a heterolysis mechanism once in contact with a proton. The specific protein environment is believed to place constraints on the H-cluster to adopt the CO-bridged conformation and

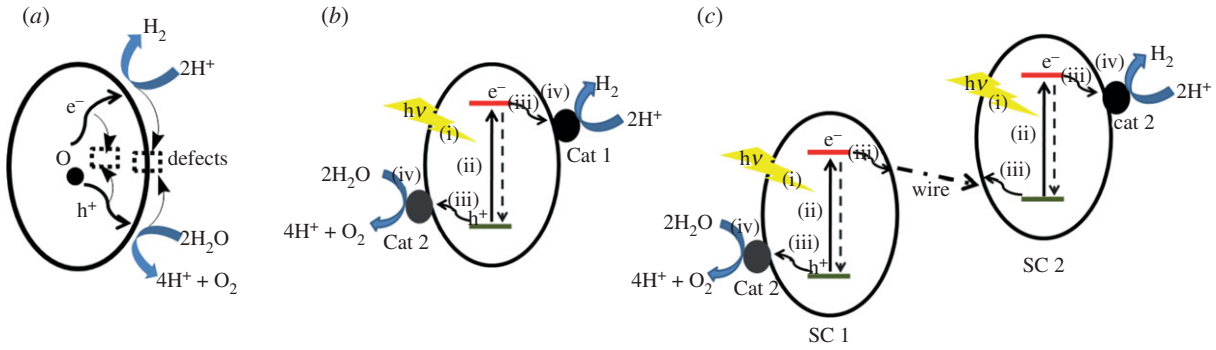

Figure 8. Schematic of how semiconducting materials can be used as photocatalysts for water oxidation and hydrogen generation. Large band gap semiconductors can be used without (*a*) or with electrocatalysts Cat1 and Cat2 (*b*). Two narrow band gap semiconductors could be wired in a Z-scheme tandem configuration (*c*).

avoid the tautomerization of terminal hydride into the more thermodynamically stable bridged hydride isomer [60]. This could well be the main reason for the impressive catalytic activities of [FeFe]-hydrogenase for hydrogen evolution with TOF up to 9000 s^{-1} [61].

In the case of [NiFe]-hydrogenases, the protonation site could be sulfur atoms of cysteine ligands, either bridged or terminal, and the redox platform was proposed to be located on the Ni^{II} centre rather than on Fe^{II}. Details of the proposed mechanistic cycle for proton reduction in this enzyme can be found in recent reviews [55,57,58,62].

The hydrogenases have been investigated as an alternative to platinum in an electrolyser and in a proton exchange membrane fuel cell [63]. However, scaling up the application of hydrogenases for catalysis technology is not practical given its oxygen sensitivity, the requirement for large-scale cultivation of organisms and difficulties in isolation of active enzyme and the overall lack of robustness for long-term operation. Nevertheless, because hydrogenases are highly catalytically active and use metals that are abundant in the Earth's crust (Fe and Ni), there are considerable efforts to mimic these enzymes by the synthesis of molecular catalysts. Indeed, considerable progress has been made with this challenge and several functional organometallic catalysts containing Ni, Fe and/or Co have been reported that show structural and/or functional features similar to those of the hydrogenases catalytic sites [64–67]. Some of these have been integrated within photo-activated systems for hydrogen generation [65–67]. We will discuss these successes in more detail in §4.

4. Artificial photosynthesis

While some progress has been made in mimicking photosynthesis in artificial systems, researchers have not yet developed components that are both efficient and robust for incorporation into a working system for capturing and storing solar energy in chemical bonds on a large scale as does natural photosynthesis. To date, the main focus has been to design and synthesize electrocatalysts that can be linked to a light-driven charge separation system [68]. Dyes have been used for the latter, but inorganic semiconductors offer a more realistic and robust approach for providing the oxidizing and/or reducing potentials necessary to split water and power reductive chemistry. Indeed, rational engineering of semiconductors to efficiently capture and stabilize the energy of solar radiation for driving multi-electron chemistry is currently a great challenge of material sciences.

In the following sections, we first discuss the design and use of semiconductors as a simple photocatalyst for water-splitting and hydrogen-generation processes. Hydrogen can be used directly as a fuel but also used to reduce CO_2 to formic acid or carbon monoxide as precursors for higher molecular weight carbon compounds as discussed by Benson *et al*. [69]. Although the generation of high-energy carbon containing fuels, such as methanol is desirable, the multi-electron nature of the CO_2-reduction process adds additional complexity compared with that for hydrogen production [68] and in this study, we restrict ourselves to latter fuel. In so doing, we discuss how an electrocatalyst could be linked to a semiconductor to enhance or promote the chemical reactions on the semiconductor surface. We end by considering the possibilities of integrating separated components (photocatalyst/photoelectrode) into a complete device that can split water into oxygen and hydrogen using only photon energy. Even though there have been demonstration systems, there remains the challenge of scaling up to a meaningful levels and reaching conversion efficiencies of at least 10 per cent.

4.1. Semiconductor: simple artificial photocatalyst

Semiconductors with the appropriate electronic properties can capture solar photons by charge separation between their valence and conduction bands, thus generating the power required for driving chemical reactions at their surfaces. In this way, a semiconductor functions in a similar manner to the reaction centre of natural photosynthesis (figure 2 and figure 8*a*). There are some semiconductors that on illumination can provide sufficient electrochemical potential to drive the water oxidation and/or proton-reduction reactions without the requirement of an electrocatalyst. Moreover, being inorganic materials means that they are usually photochemically stable that make them good candidates for developing robust technology for large-scale solar fuel production.

Since the pioneering work reported by Fujishima & Honda [70] using a TiO_2 photoanode for water splitting, several families of semiconductor have been investigated. They include metal oxides (Cu_2O, TiO_2, Fe_2O_3, WO_3, $BiVO_4$), metal sulfides (CdS, CdZnS) and chalcopyrites (CuInS, CuGaS) [71,72]. Large band gap semiconductors (more than 3 eV) such as TiO_2 and graphitic carbon nitride g-C_3N_4 can be suitable for driving the overall water-splitting process. However, these materials absorb only UV and near-to-UV light, which is a small portion

of the solar spectrum at the Earth's surface. Considerable efforts are currently underway to extend the absorption of these materials to the visible light region. Elemental doping, rational nanostructuring and surface functionalization are among the strategies to induce appropriate absorption shifts to longer wavelengths [73–75].

Narrow band gap materials such as Fe_2O_3 (2.2 eV) and Cu_2O (2.0–2.2 eV) match well with the absorption of visible light. However, the energies of their valence and conduction bands are usually not appropriate for driving the overall water-splitting process to generate both molecular O_2 and H_2 at the same time. Some of them, for example α-Fe_2O_3, have their conduction band energies lying at a more positive potential than the reduction potential required to convert protons to hydrogen, whereas others, e.g. Cu_2O, have the energy of their valence bands positioned at more negative potentials than required for water oxidation. Consequently, these materials can be used only for the half-reaction: either photo-driven water oxidation or hydrogen evolution. To construct a complete system for the overall water-splitting process, the two matching narrow band gap materials must be wired in a tandem configuration (figure 8*c*) akin to PSII and PSI in the Z-scheme (figure 2). In this case, as with natural photosynthesis, the energy of two photons is required for each overall electron transfer, thus decreasing the efficiency of the charge separation reaction by 50 per cent. Another issue concerning narrow band gap semiconductors being studied at the moment is their photochemical instability. Nevertheless, rational nanostructuring is proving to be a valuable approach to overcome the stability problem [76,77].

It is worth mentioning that charge recombination within, and on the surface, of semiconductors can often be a key factor controlling the photo-to-energy conversion efficiency. In the reaction centres of natural photosynthesis, the recombination reactions are minimized by subsequent rapid secondary electron transfer steps. This concept of optimization of charge separation has also been successfully applied in semiconductor engineering. Charge separation within a semiconductor can be enhanced by combining with another appropriate semiconductor in a pn junction system [76] or interfacing with an electron acceptor, e.g. graphene, carbon nanotubes [77,78]. Enhancing charge separation efficiency can be addressed by dealing with the intrinsic conductivity of a semiconductor by elemental doping [79,80] or by effacing the semiconductor surface defects by applying a thin oxide layer [81–83].

To accelerate chemical reactions on the semiconductor surface, loading of an oxygen-evolving catalyst (OEC) and a catalyst for hydrogen evolution reaction (HER) is often beneficial (figure 8*b*,*c*). In these hybrid systems, the OEC and HER catalysts extract generated holes (oxidizing equivalent) and electrons (reducing equivalents) from the semiconductor and subsequently drive the water oxidation and the HER on its surface. In §4.2, we will discuss how catalysts such as enzymes and their biomimetic synthetic equivalents have been linked to semiconductors for engineering hybrid photocatalysts.

4.2. Hybrid photocatalysts for water oxidation and oxygen evolution

A dinuclear ruthenium complex (the blue dimer) was the first example of a molecular catalyst that could electrochemically split water into O_2, protons and electrons [84]. Since then, considerable efforts have been focused on designing appropriate organic ligands to improve the activity and stability of related Ru-based catalysts. The most striking success was recently reported by Sun and co-workers [85], who synthesized a super Ru-complex that catalyses the oxygen evolution reaction at a rate comparable with that of PSII.

Given that ruthenium is not an abundant metal, attention has been focused on the design and synthesis of water-splitting catalysts composed of readily available elements such as Mn, Co, Fe [66,67,86]. Remarkable advances were recently achieved by Agapie and co-worker [87] and Christou and co-worker [88] in the synthesis of Mn_3CaO_4-clusters (figure 9*a*,*b*) geometrically very closely resembling the Mn_4Ca-cluster of PSII. These PSII-mimics have yet to be investigated for any catalytic activity and almost certainly will require further modification of their coordination spheres to give stability and facilitate efficient water-splitting properties. Indeed, stability under catalytic functional conditions, at high oxidative potential, is a critical issue for all known organometallic water oxidation catalysts. To address this issue, one possible solution is to use all-inorganic catalysts that do not contain any fragile organic ligands in their structures. For example, Hill and co-workers [89] demonstrated the possibility of using polyoxometallate ligands to stabilize a O–O bond forming catalytic centre composed of a cobalt oxide core (Co_4O_4; figure 9*c*). Cobalt- and nickel-based systems, together with inorganic anionic ligands acting as good proton transfer agents, have been developed by Nocera and co-workers [90,94] and demonstrated to be very impressive catalysts for water oxidation. The cobalt-oxide-phosphate catalyst they discovered (CoPi) functions in a neutral pH solution with an overpotential of only *ca* 400 mV (figure 9*d*). Interestingly, this solid-state catalyst is made up of cubic structures with oxo-bridging, therefore showing structural similarities to the geometry of the Mn_4Ca-cluster of PSII [95,96]. A very important property of this CoPi catalyst is its ability to self-repair which is reminiscent of the property of PSII to do the same [97].

Taking a different approach, Frei & Jiao [98,99] have demonstrated that a silica scaffold is a good support for stabilizing and activating cobalt-oxide or manganese-oxide nanoparticles for water-splitting activity.

Immobilizing an OEC onto an *n*-type semiconductor surface to engineer a photoanode or a photocatalyst for water splitting can be accomplished by adopting several different strategies. Organometallic molecular catalysts can be simply absorbed via a physical process [100,101] or covalently grafted via a robust chemical linker (figure 10*a*) [102,103]. The latter approach usually requires a complicated and expensive synthesis to introduce appropriate grafting anchors to the catalyst [108]. However, such systems are likely to be more robust compared with those relying on physical adsorption, thanks to the stabilizing effect of having a linker present.

In the case of inorganic-based OEC catalysts, physical adsorption onto the semiconductor surface can be very satisfactory. For example, by taking this approach, it was reported that spinel Co_3O_4 nanoparticles were homogeneously incorporated within a mesoporous g-C_3N_4 matrix resulting in an efficient Co_3O_4/g-C_3N_4 photocatalyst [109]. Alternatively, spinel Co_3O_4 catalyst can be directly co-grown with the α-Fe_2O_3 nanowires via a hydrothermal process (figure 10*b*) [104]. However, electrodeposition and photo-assisted

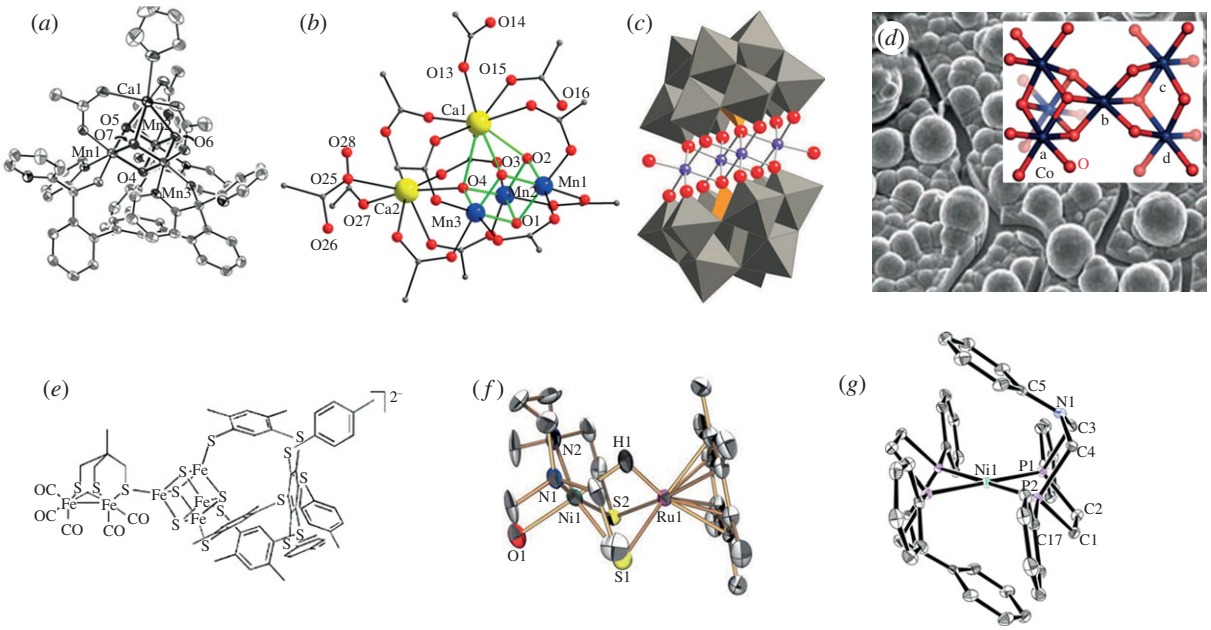

Figure 9. Selected synthetic electrocatalysts that mimic the [Mn_4Ca]-cluster and the active sites of hydrogenases. Synthetic [Mn_3CaO_4]-clusters designed by Agapie and co-workers (*a*) [87] and Christou and co-workers (*b*) [88]; Co_4O_{16} core stabilized within [PW_9O_{34}] ligand synthesized by Hill and co-workers (*c*) [89]; Nocera CoPi solid catalyst and its proposed atomic structure (*d*) [90]; synthetic [FeFe] and [NiFe] models designed by Pickett and co-workers [91] and Ogo and co-workers [92] (*e*) and (*f*); bioinspired model designed by Dubois and co-workers (*g*) [93].

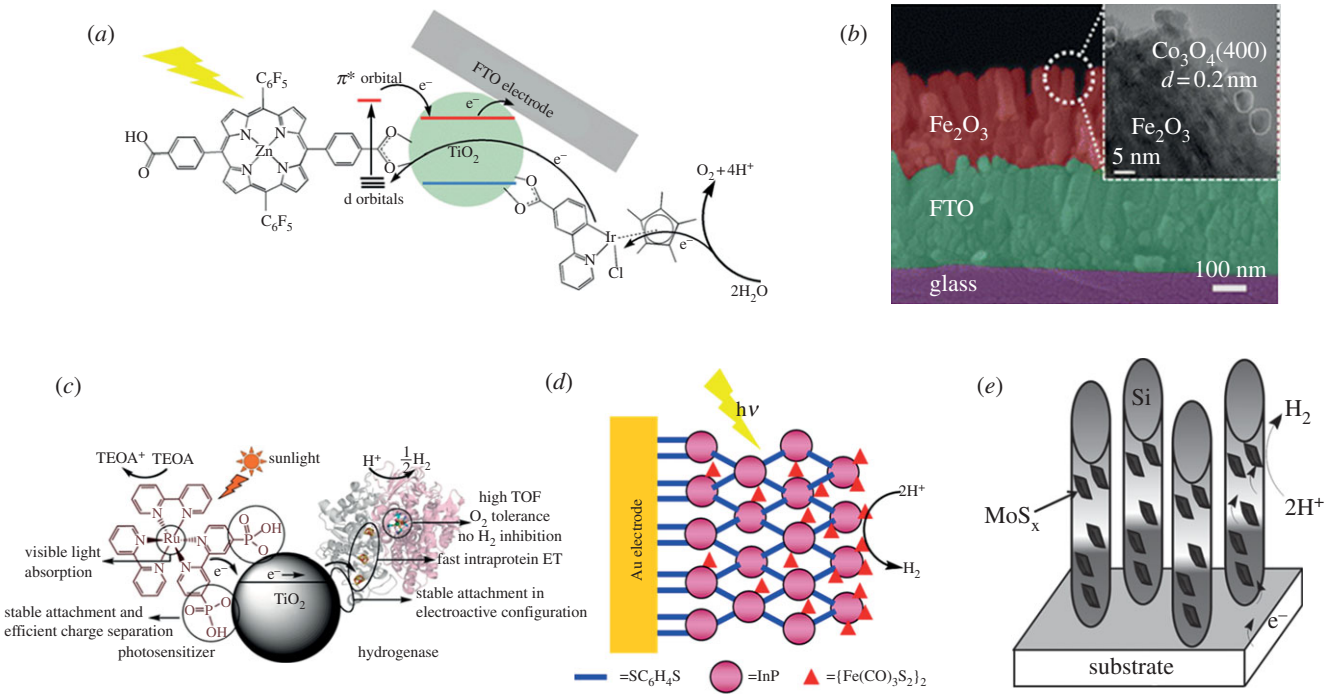

Figure 10. Selected hybrid photocatalysts/photoelectrodes engineered by assembling an OEC or a HER catalyst with a semiconductor. Ir-molecular OEC catalyst covalently grafted onto a dye-sensitized TiO_2 electrode (*a*) [102,103]; Co_3O_4 OEC within α-Fe_2O_3 nanowires photoanode (*b*) [104]; immobilization of a [NiFeSe]-hydrogenase onto dye-sensitized TiO_2 nanoparticles (*c*) [105]; immobilization of a synthetic FeFe-molecular HER catalyst within a mesoporous InP electrode (*d*) [106]; Si/MoS_2 photocathode (*e*) [107].

electrodeposition seem to be a better approach to introduce cobalt-oxide-based catalysts onto the surface of photoanodes such as Fe_2O_3, ZnO, WO_3 [110–112]. There is evidence that the photo-assisted method provides a well-controlled deposition of CoPi for the construction of a photoanode. For example, a better performance was achieved for a α-Fe_2O_3/CoPi when using photo-assisted electrodeposition compared with a α-Fe_2O_3/CoPi electrodeposition [110].

Despite successes with cobalt-oxide-based catalysts deposited in nanoparticles form, they suffer from not having a robust linker to the semiconductor surface. Thus, during catalytic turnover with the production of O_2 bubbles at the surface, detachment of these catalysts can occur over time. Introducing a covalent linker, as in the case of molecular organo-metallic catalysts, is unlikely to be a credible solution because chemical functionalization changes the

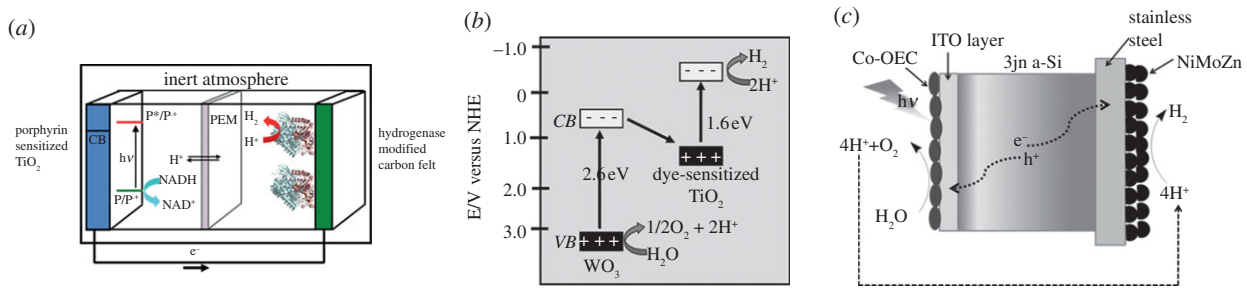

Figure 11. Selected complete devices for the overall water-splitting process. A PEC consisted of a dye-sensitized TiO_2 photoanode and a hydrogenase cathode (*a*) [119]; a PEC with two photoelectrodes in the tandem configuration (*b*) [120]; the artificial leaf constructed from an amorphous Si triple junction solar cell and appropriate OEC and HER catalysts (*c*) [121,122].

surface properties of nanoparticles and therefore likely to change their catalytic activities. Therefore, a system that is self-repairing under functional conditions is ideal as in the case of the Nocera CoPi OEC catalyst.

4.3. Hybrid photocatalysts for proton reduction and hydrogen evolution

An example of integrating isolated natural hydrogenase within a photocatalytic system was demonstrated by Armstrong and co-workers [105] when they immobilized a [NiFeSe]-hydrogenase from *Desulfomicrobium baculatum* on to the surface of Ru-dye-sensitized TiO_2 nanoparticles (figure 10*c*). This photocatalyst produced H_2 when illuminated with visible light in the presence of a sacrificial electron donor. However, owing to the large geometric size of hydrogenases, the level of loading onto the semiconductor surface was low, thus limiting the efficiency of this approach. Moreover, as mentioned earlier, the instability of this class of isolated enzymes and their sensitivity to oxygen, makes this biological approach unlikely for technological advancement. In addition, the requirement for large quantities of isolated enzyme is not conducive for a technology to produce solar fuel at worthwhile levels.

A possible solution is to use small and more robust molecular catalysts (figure 9*e–g*) [91–93] that mimic the catalytic active site of the hydrogenases and hybridize them with a p-type semiconductor. As in the case of molecular OEC, the hybridization could be accomplished by either a non-covalent or a covalent grafting. The first demonstration of this approach was reported by Nann *et al*. [106] when they adsorbed a $Fe_2S_2(CO)_6$, the simplest mimicking equivalent of the [FeFe]-hydrogenase, with a mesoporous p-type InP photoelectrode (figure 10*d*). Cobaloxime, a bioinspired equivalent of hydrogenases, was also successfully integrated with an organic dye-sensitized-NiO or a Ru-dye-sensitized TiO_2 electrode via either non-covalent [113] or covalent grafting [114]. However, these photocathodes showed moderate efficiency; typical photocurrents of only a few microamperes were obtained. Several reasons can explain this low photon-to-energy conversion efficiency, including moderate photo-to-current conversion of a dye-sensitized electrode interfacing with an aqueous solution,[1] low overpotential provided by the conduction band of TiO_2 and low electrocatalytic activities of FeFe or cobaloxime catalyst in aqueous solution, especially in weak acidic conditions.

Therefore, further efforts are required to address the low activities of synthetic molecular HER catalysts in aqueous, near-to-neutral pH solution. Covalently grafting these molecular catalysts onto a visible light-absorbing p-type semiconductor, such as Cu_2O or CuInS(Se) could be of interest, because these semiconductors provide large reductive potential (thanks to their favourable conduction band energies).

While using hydrogenases and their mimics are still in the very early stages of proof-of-concept, all-inorganic HER electrocatalysts seem to be better candidates for interfacing with appropriate semiconductors. Nanoclusters of Ni, Co and their alloys with molybdenum were demonstrated to be potential electrocatalysts for HER [116,117]. Interfacing NiMo alloy nanoparticles with Si microarrays resulted in an effective photocathode that produced impressive photocurrents in the region of 15 mA cm^{-2} at 0 V versus reversible hydrogen electrode (RHE) powered by one Sun illumination [118]. Recently, NiMoZn was used for construction of the Si triple junction artificial leaf (see §4.4 and figure 11*c*) [121]. The chemical dissolution of Mo in an alkaline solution resulted in production of highly porous and thus, highly active NiMoZn catalyst.

Recently, MoS_2 has emerged as one of the most promising noble-metal-free electrocatalysts for HER. This catalyst functions over a wide range of pH solutions (pH 0–13) with low over-potential requirement (*ca* 100–200 mV) [123,124]. It can be introduced to a semiconductor surface via a thermal deposition [125], electrodeposition [126] or a photo-assisted deposition process [107]. On a Si nanowire electrode or on CdS nanopowder surface, MoS_2 is as efficient as Pt nanoparticles for hydrogen photogeneration (figure 10*e*) [107,125]. Moreover, MoS_2 is chemically and photochemically stable, thus making the engineering of a robust photocatalyst/photoelectrode feasible.

4.4. Constructing a complete photocatalytic system for oxygen and hydrogen generation from water

The ultimate goal of artificial photosynthesis research is to construct a viable photocatalyst or photocatalytic system that can convert solar irradiation into hydrogen via the water-splitting process without the requirement of any external bias. To date, only a few examples of such systems have been reported and all still function with low solar-to-fuel conversion efficiency. These systems can be divided into three main classes: (i) suspended nanopowder photocatalysts, (ii) photoelectrochemical cells (PECs), and (iii) photovoltaic cell-driven electrolysers.

(i) As mentioned above, some large band gap semiconductors such as TiO_2 or g-C_3N_4 can split water into oxygen

and hydrogen under UV or near-to-UV illumination without requirement of any electrocatalyst. Introducing an OEC and/or HER catalyst on the surface of these semiconductors enhances their photocatalytic activities. These electrocatalysts act as traps for electrons and holes as well as enhancing the rates of the chemical reactions. However, co-loading of two electrocatalysts on the same semiconductor is technically challenging. Moreover, almost all types of HER catalysts, e.g. hydrogenase, synthetic molecular organo-metallic and inorganic catalysts, are not usually stable under high oxidative potentials. By contrast, almost all OECs, such as CoPi, are not stable under high reductive potential. This stability issue can be addressed by using noble metal oxide catalysts that are robust under both reductive and oxidative conditions such as $Rh_{2-y}Cr_yO_3$ and RuO_2 [127,128]. However, the noble metal oxides are not abundant and therefore are expensive. An alternative approach has recently emerged involving the use of single metal oxide catalysts. Domen and co-workers [129] reported that a NiO_x-loaded-$SrTiO_3$ acted as an artificial photocatalyst for the overall water-splitting process producing both oxygen and hydrogen on illumination. Recent investigations revealed that some of NiO_x is reduced by electrons generated in the conduction band of $SrTiO_2$ resulting in Ni^0 clusters [117]. Therefore, the $NiO_x/SrTiO_3$ system was converted *in situ* into $NiO_x/SrTiO_3$/Ni nanoscale 'artificial leaf' in which Ni acts as a HER catalyst, whereas NiO_x acts as an OEC. A similar inter-conversion between OEC and HER activities governed by oxidizing or reducing potential could also allow a cobalt-oxide-phosphate system to function in a single device [130].

Another approach is to use oxygen- and hydrogen-producing electrocatalysts deposited onto two different semiconductors and 'wired' into a complete photocatalytic system for the overall water-splitting process (figure 11*a*). By doing this, two low-energy semiconductors can be used in a tandem configuration (figure 8*c*). The two nanopowder photocatalysts would be electrically connected by either a hard wire (a solid wire such as graphene sheet) [131] or a soft-wire (a soluble redox couple such as IO_3^-/I^-) [132–134]. In principle, by using a soluble electron shuttle, it is possible to separate water oxidation photocatalysts and hydrogen evolution photocatalysts into two compartments. Such an arrangement allows the separating of H_2 and O_2 products that is not possible when using a single large band gap semiconductor with HER and OEC catalysts co-loaded. Indeed, production of a H_2/O_2 mixture is not ideal for large-scale application for safety reasons.

(ii) PEC system. A PEC cell for water-splitting application should contain a photoanode for extracting electrons from water using solar irradiation as the energy source and a photocathode or a cathode to use these reductive electrons for the hydrogen-generation reaction. The ideal cathode material is platinum and it was used by Fujishima & Honda [70] in their classic work with TiO_2. As stated earlier, hydrogenase is an electrocatalyst as active as Pt [56]. Indeed, an effective PEC was constructed by Moore *et al.* [119] using a hydrogenase-decorated carbon fibre electrode with a dye-sensitized TiO_2 photoanode (figure 11*a*). Both Pt and hydrogenase function with near-to-zero over-potential requirement. As a result, electrons in the TiO_2 conduction band possess enough reductive potential for the HER with these catalysts. However, to replace the Pt or hydrogenase by a robust electrocatalyst engineered from abundant chemicals such as NiP_4 [135], MoS_2 [124] or Cu_2MoS_4 [136], a photoanode material that possesses a more negative conduction band is required. Examples on such designs have not yet been reported.

Alternatively, low-energy conduction band photoanodes can be wired to a photocathode in a tandem configuration (figure 11*b*) [120]. By doing so, electrons generated by the photoanode can be further energized by the photocathode so as to provide enough reductive potential to power platinum-free or hydrogenase-free HER electrocatalysis leading to hydrogen production. To make full use of the visible spectrum, a blue-light-absorbing material should ideally be used for the photoanode while the photocathode should be made of a red-light-absorbing material. The two electrodes can be on opposite sides of a proton transfer membrane, e.g. Nafion, and thus allow separation of H_2 and O_2 products as well as managing proton transportation from the photoanode to the (photo)cathode. In principle, with a proton exchange membrane, it should be possible to engineer a PEC cell with two compartments at different pHs. Indeed, in general, an alkaline solution is preferred for anodic function, whereas acidic solution is preferred for cathodic reactions. However, with the perspective of a large-scale solar hydrogen production, a PEC with two electrodes functioning in neutral or near-to-neutral pH solutions, and if possible with sea water, is desirable. To this end, further efforts are needed to improve the activities of current photoelectrode materials as well as electrocatalysts. At the current stage of development, several potential photoanodes and photocathodes are being investigated as separate entities. The ultimate goal is to screen these systems for the possibility of combining them into a fully assembled PEC device along the lines described below.

(iii) Photovoltaic-electrolyser combination. Coupling a Si solar cell or a dye-sensitized solar cell to an electrolyser could be a possible technological solution to initially convert solar radiation into electricity and then use this electrical energy to split water into hydrogen and oxygen via classical electrolysis. It is still not clear whether this configuration is more efficient than a photocatalyst or a PEC type system and whether cost and practical considerations will identify the most effective route for solar fuel production on a large scale.

Rocheleau *et al.* [122] and more recently Nocera and co-workers [121] reported a relatively simple PEC system that effectively used sunlight to split water into oxygen and hydrogen. This 'artificial leaf' was constructed by direct deposition of two electrocatalysts onto the sides of an amorphous triple junction Si solar cell (figure 11*c*). The OEC, consisting of either a $NiFe_xO_y$ or CoPi catalyst, was deposited onto a ITO layer on one surface of Si wafer, whereas the HER catalyst, a CoMo alloy or NiMoZn, was assembled on steel plate in contact with the other side of the Si wafer. On illuminating the Si solar cell, charge separation occurred within the triple junction cell. The positive holes in the valence band extracted electrons from water with the aid of the OEC. The negative charges present in the conduction band were transferred into the HER catalyst to mediate the reduction of protons into hydrogen. Although not fully optimized, these two examples of a working 'artificial leaf' system had an overall photon-to-hydrogen conversion efficiency of *ca* 7.8 per cent [122]. These two examples were also demonstrated to be robust under outdoor test conditions for thousands of hours. Although it is still early days, these devices represent

a significant advance in the ultimate goal to engineer a robust artificial photosynthetic system composed of Earth's abundant elements to harvest and convert sunlight into hydrogen with a desired efficiency of 10 per cent or more.

5. Conclusions

It is anticipated that the global demand for energy will more than double by the mid-century and perhaps more than triple by the end of the century. Satisfying this demand will be necessary in order to achieve vibrant technological progress, economic growth and most importantly, political stability over the coming decades. Already we are faced with the prospect of catastrophic climate change owing to the release of CO_2 into the atmosphere brought about by the burning of fossil fuels. In the short-term, we must exploit all technologies known to us to produce energy while at the same time reduce CO_2 emission. The nature of mix of the approaches adopted will vary between different countries depending on their resources and populations with some dominating factors (e.g. geothermal in Iceland, biomass in Brazil, etc.). Coupled with this, challenge is to use energy more efficiently. Here again, we can learn from nature. In biology, the 'combustion' of fuel (food) is accomplished isothermally by highly efficient and subtle biological reactions involving a host of clever enzymes. For example, when the 'hydrogen' of glucose is combined with oxygen during the process of respiration to produce water and CO_2, about 30 ATP molecules are made. ATP is the energy currency of cells. Because ATP stores 12 kcal per mole (50 kJ mol^{-1}) of usable energy and the energy content of glucose is 673 kcal per quantum mole (2805 kJ $mole^{-1}$), the efficiency of energy conversion is in the region of 54 per cent. It therefore seems to us that mankind should learn from biology's example and strive to develop new technologies that are as energy efficient as natural enzymes.

For the long term, we will have very few options to replace fossil fuels and satisfy the increased energy demands of a global population of 10 billion or more. Renewables such as hydropower, wind, wave, geothermal and biomass will not be able to supply energy equivalent to 20 TW even when taken together [4]. Nuclear fission is a short-term solution but in the long-run will probably not be a realistic option. Nuclear fusion is a possibility but the construction of a working reactor is proving problematic. Nevertheless, we must continue to explore this potential technology with the hope that it will come on stream sooner or later. However, there is another nuclear reaction that is already up and running, namely the Sun. Our sun is the champion of energy sources: delivering more energy to the Earth in an hour than we currently use in a year from fossil, nuclear and all renewable sources combined. Its energy supply is inexhaustible in human terms, more or less evenly distributed globally and its use is harmless to our environment and climate.

The enormous untapped potential of solar energy is an opportunity that should be addressed with urgency. Biology chose this energy source, and there is no reason why the chemical reactions devised by photosynthetic organisms cannot be mimicked by the ingenuity of humans. We already have a considerable knowledge base and the emerging nanotechnologies to exploit. With a concerted input of the talents of scientists trained in different disciplines, it should be possible to move the technologies of solar energy capture and storage forward. The recognition of Manhattan- or Apollo-like initiatives to develop new sustainable energy technologies in response to the CO_2 problem as suggested by Hoffert *et al*. [2] should be the driver for encouraging basic and applied research in this area. As outlined in this study, significant progress is being made although the overall challenge to go from micro- to macroscale should not be underestimated.

Endnote

[1]In a Graetzel solar cell, the dye-sensitized TiO_2 electrode is interfaced with acetonitrile or an ionic liquid solution and the holes generated are efficiently quenched by I^- [115].

References

1. International Energy Agency. 2012 *Key World Energy Statistics 2012*. Paris, France: International Energy Agency. (http://www.iea.org)
2. Hoffert MT *et al*. 1998 Energy implications of future stabilization of atmospheric CO_2 content. *Nature* **395**, 881–884. (doi:10.1038/27638)
3. Nakicenovic N, Swart R. 2000 *Special report on emissions scenarios*, pp. 48–55. Washington, DC: Intergovernmental Panel on Climate Change.
4. Lewis NS, Nocera DG. 2006 Powering the planet: chemical challenges in solar energy utilization. *Proc. Natl Acad. Sci. USA* **103**, 15 729–15 735. (doi:10.1073/pnas.0603395103)
5. United Nations Development Program 2003 *World energy assessment report: energy and the challenge of sustainability*. New York, NY: United Nations.
6. Pachauri R, Reisinger A. 2007 Contribution of working groups I, II, and III to the fourth assessment. Report of the Intergovernmental Panel on Climate Change. In *Climate change 2007, synthesis report* (eds Core Writing Team, Bernstein *et al*.), Geneva, Switzerland: IPCC. See http://www.ipcc.ch/pdf/assessment-report/ar4/syr/ar4_syr.pdf.
7. Metz B, Davidson O, de Coninck H, Loos M, Meyer L. 2005 *Carbon dioxide capture and storage*. Cambridge, UK: Intergovernmental Panel on Climate Change, Cambridge University Press.
8. Solar Energy Utilization Workshop 2005 *Basic science needs for solar energy utilization*. Washington, DC: US Department of Energy.
9. Shaheen SE, Ginley DS, Jabbour GE. 2005 Organic-based photovoltaics toward low-cost power generation. *MRS Bull.* **30**, 10–19. (doi:10.1557/mrs2005.2)
10. Hagberg DP *et al*. 2008 Molecular engineering of organic sensitizers for dye-sensitized solar cell applications. *J. Am. Chem. Soc.* **130**, 6259–6266. (doi:10.1021/ja800066y)
11. Thorndike EH. 1996 *Energy and the environment*. Reading, MA: Addison-Wesley.
12. Walker DA. 1977 *Energy, plants and man*. Chichester, UK: Packard Publishing Ltd.
13. Archer MD, Barber J. 2004 Photosynthesis and photoconversion. In *Molecular to global photosynthesis* (eds MD Archer, J Barber), pp. 1–41. London, UK: Imperial College Press.
14. Bolton JR, Hall DO. 1991 The maximum efficiency of photosynthesis. *Photochem. Photobiol.* **53**, 545–548. (doi:10.1111/j.1751-1097.1991.tb03668.x)
15. Blankenship RE *et al*. 2011 Comparing photosynthetic and photovoltaic efficiencies and recognizing the potential for improvement. *Science* **332**, 805–809. (doi:10.1126/science.1200165)
16. Falkowsky PG, Raven JA. 1997 *Aquatic photosynthesis*. Oxford, UK: Blackwell.

17. Blankenship RE. 2002 *Molecular mechanisms of photosynthesis*. Oxford, UK: Blackwell Science.
18. Barber J, Andersson B. 1994 Revealing the blueprint of photosynthesis. *Nature* **370**, 31–34. (doi:10.1038/370031a0)
19. Schubert W-D, Klukas O, Saenger W, Witt HT, Fromme P, Krauß N. 1998 A common ancestor for oxygenic and anoxygenic photosynthetic systems: a comparison based on the structural model of photosystem I. *J. Mol. Biol.* **280**, 297–314. (doi:10.1006/jmbi.1998.1824)
20. Rhee K-H, Morris EP, Barber J, Kuhlbrandt W. 1998 Three-dimensional structure of the photosystem II reaction center at 8 Å resolution. *Nature* **396**, 283–286. (doi:10.1038/24421)
21. van Amerongen H, Valkunas L, van Grondelle R. 2000 *Photosynthetic excitons*. Singapore: World Scientific.
22. Barber J. 2003 Photosystem II: the engine of life. *Q. Rev. Biophys.* **36**, 71–89. (doi:10.1017/S0033583502003839)
23. Wydrzynski TJ, Satoh K. 2005 Photosystem II: the light-driven water: plastoquinone oxidoreductase. In *Advances in photosynthesis and respiration*, vol. 22, pp. 1–786. Dordrecht, The Netherlands: Springer.
24. Barber J, Rutherford AW. 2008 Revealing how nature uses sunlight to split water. *Phil. Trans. R. Soc. B* **363**, 1125–1128. (doi:10.1098/rstb.2007.2227)
25. Yano J *et al*. 2006 Where water is oxidized to dioxygen: structure of the photosynthetic Mn_4Ca cluster. *Science* **314**, 821–825. (doi:10.1126/science.1128186)
26. Sauer K, Yano J, Yachandra VK. 2008 X-ray spectroscopy of the photosynthetic oxygen-evolving complex. *Coord. Chem. Rev.* **252**, 318–335. (doi:10.1016/j.ccr.2007.08.009)
27. Yano J, Yachandra VK. 2008 Where water is oxidized to dioxygen: structure of the photosynthetic Mn_4Ca cluster from X-ray spectroscopy. *Inorg. Chem.* **47**, 1711–1726. (doi:10.1021/ic7016837)
28. Zouni A, Witt HT, Kern J, Fromme P, Krauss N, Saenger W, Orth P. 2001 Crystal structure of photosystem II from *Synechococcus elongatus* at 3.8 Å resolution. *Nature* **409**, 739–743. (doi:10.1038/35055589)
29. Kamiya N, Shen J-R. 2003 Crystal structure of oxygen-evolving photosystem II from *Thermosynechococcus vulcanus* at 3.7 Å resolution. *Proc. Natl Acad. Sci. USA* **100**, 98–103. (doi:10.1073/pnas.0135651100)
30. Ferreira KN, Iverson TM, Maghlaoui K, Barber J, Iwata S. 2004 Architecture of the photosynthetic oxygen-evolving center. *Science* **303**, 1831–1838. (doi:10.1126/science.1093087)
31. Loll B, Kern J, Saenger W, Zouni A, Biesiadka J. 2005 Towards complete cofactor arrangement in the 3.0 Å resolution structure of photosystem II. *Nature* **438**, 1040–1044. (doi:10.1038/nature04224)
32. Umena Y, Kawakami K, Shen J-R, Kamiya N. 2011 Crystal structure of oxygen-evolving photosystem II at a resolution of 1.9 Å. *Nature* **473**, 55–60. (doi:10.1038/nature09913)
33. Sproviero EM, Gascon JA, McEvoy JP, Brudvig GW, Batista VS. 2006 QM/MM models of the O_2-evolving complex of photosystem II. *J. Chem. Theory Comput.* **2**, 1119–1134. (doi:10.1021/ct060018l)
34. Sproviero EM, Gascon JA, McEvoy JP, Brudvig GW, Batista VS. 2007 Quantum mechanics/molecular mechanics structure models of the oxygen-evolving complex of photosystem II. *Curr. Opin. Struct. Biol.* **17**, 173–180. (doi:10.1016/j.sbi.2007.03.015)
35. Sproviero EM, Gascón JA, McEvoy JP, Brudvig GW, Batista VS. 2008 Quantum mechanics/molecular mechanics study of the catalytic cycle of water splitting in photosystem II. *J. Am. Chem. Soc.* **130**, 3428–3442. (doi:10.1021/ja076130q)
36. Messinger J, Badger M, Wydrzynski T. 1995 Detection of one slowly exchanging substrate water molecule in the S3 state of photosystem II. *Proc. Natl Acad. Sci. USA* **92**, 3209–3213. (doi:10.1073/pnas.92.8.3209)
37. Pecoraro VL, Baldwin MJ, Caudle MT, Hsieh WY, Law NA. 1998 A proposal for water oxidation in photosystem II. *Pure Appl. Chem.* **70**, 925.
38. McEvoy JP, Brudvig GW. 2004 Structure-based mechanism of photosynthetic water oxidation. *Phys. Chem. Chem. Phys.* **6**, 4754–4763. (doi:10.1039/b407500e)
39. McEvoy JP, Brudvig GW. 2006 Water-splitting chemistry of photosystem II. *Chem. Rev.* **106**, 4455–4483. (doi:10.1021/cr0204294)
40. Sproviero EM, Gascón JA, McEvoy JP, Brudvig GW, Batista VS. 2008 Computational studies of the O_2-evolving complex of photosystem II and biomimetic oxomanganese complexes. *Coord. Chem. Rev.* **252**, 395–415. (doi:10.1016/j.ccr.2007.09.006)
41. Siegbahn PEM. 2006 O–O bond formation in the S4 state of the oxygen-evolving complex in photosystem II. *Chem. Eur. J.* **12**, 9217–9227. (doi:10.1002/chem.200600774)
42. Siegbahn PEM. 2009 Structures and energetics for O_2 formation in photosystem II. *Accounts Chem. Res.* **42**, 1871–1880. (doi:10.1021/ar900117k)
43. Siegbahn PEM. 2012 Mechanisms for proton release during water oxidation in the S2 to S3 and S3 to S4 transitions in photosystem II. *Phys. Chem. Chem. Phys.* **14**, 4849–4856. (doi:10.1039/c2cp00034b)
44. Kok B, Forbush B, McGloin M. 1970 Cooperation of charges in photosynthetic O_2 evolution-I. A linear four step mechanism. *Photochem. Photobiol.* **11**, 457–475. (doi:10.1111/j.1751-1097.1970.tb06017.x)
45. Gatt P, Petrie S, Stranger R, Pace RJ. 2012 Rationalizing the 1.9 Å crystal structure of photosystem II. A remarkable Jahn–Teller balancing act induced by a single proton transfer. *Angew. Chem. Int. Ed.* **51**, 12 025–12 028. (doi:10.1002/anie.201206316)
46. Kolling DRJ, Cox N, Ananyev GM, Pace RJ, Dismukes GC. 2012 What are the oxidation states of manganese required to catalyze photosynthetic water oxidation? *Biophys. J.* **103**, 313–322. (doi:10.1016/j.bpj.2012.05.031)
47. Isobe H, Shoji M, Yamanaka S, Umena Y, Kawakami K, Kamiya N, Shen J-R, Yamaguchi K. 2012 Theoretical illumination of water-inserted structures of the $CaMn_4O_5$ cluster in the S2 and S3 states of oxygen-evolving complex of photosystem II: full geometry optimizations by B3LYP hybrid density functional. *Dalton Trans.* **41**, 13 727–13 740. (doi:10.1039/c2dt31420g)
48. Kusunoki M. 2011 S1-state Mn_4Ca complex of photosystem II exists in equilibrium between the two most-stable isomeric substates: XRD and EXAFS evidence. *J. Photochem. Photobiol. B Biol.* **104**, 100–110. (doi:10.1016/j.jphotobiol.2011.03.002)
49. Rapatskiy L *et al*. 2012 Detection of the water-binding sites of the oxygen-evolving complex of photosystem II using W-Band 17O electron–electron double resonance-detected NMR spectroscopy. *J. Am. Chem. Soc.* **134**, 16 619–16 634. (doi:10.1021/ja3053267)
50. Ames W, Pantazis DA, Krewald V, Cox N, Messinger J, Lubitz W, Neese F. 2011 Theoretical evaluation of structural models of the S2 state in the oxygen evolving complex of photosystem II: protonation states and magnetic interactions. *J. Am. Chem. Soc.* **133**, 19 743–19 757. (doi:10.1021/ja2041805)
51. Volbeda A, Charon M-H, Piras C, Hatchikian EC, Frey M, Fontecilla-Camps JC. 1995 Crystal structure of the nickel-iron hydrogenase from *Desulfovibrio gigas*. *Nature* **373**, 580–587. (doi:10.1038/373580a0)
52. Peters JW, Lanzilotta WN, Lemon BJ, Seefeldt LC. 1998 X-ray crystal structure of the Fe-only hydrogenase (CpI) from *Clostridium pasteurianum* to 1.8 Å resolution. *Science* **282**, 1853–1858. (doi:10.1126/science.282.5395.1853)
53. Nicolet Y, Piras C, Legrand P, Hatchikian CE, Fontecilla-Camps JC. 1999 *Desulfovibrio desulfuricans* iron hydrogenase: the structure shows unusual coordination to an active site Fe binuclear center. *Structure* **7**, 13–23. (doi:10.1016/S0969-2126(99)80005-7)
54. Zirngibl C, Van Dongen W, Schworer B, Von Bunau R, Richter M, Klein A, Thauer RK. 1992 H_2-forming methylenetetrahydromethanopterin dehydrogenase, a novel type of hydrogenase without iron-sulfur clusters in methanogenic archaea. *Eur. J. Biochem.* **208**, 511–520. (doi:10.1111/j.1432-1033.1992.tb17215.x)
55. Fontecilla-Camps JC, Volbeda A, Cavazza C, Nicolet Y. 2007 Structure/function relationships of [NiFe]- and [FeFe]-hydrogenases. *Chem. Rev.* **107**, 4273–4303. (doi:10.1021/cr050195z)
56. Jones AK, Sillery E, Albracht SPJ, Armstrong FA. 2002 Direct comparison of the electrocatalytic oxidation of hydrogen by an enzyme and a platinum catalyst. *Chem. Commun.* **2002**, 866–867. (doi:10.1039/B201337A)
57. De Lacey AL, Fernández VM, Rousset M, Cammack R. 2007 Activation and inactivation of hydrogenase function and the catalytic cycle: spectroelectrochemical studies. *Chem. Rev.* **107**, 4304–4330. (doi:10.1021/cr0501947)
58. Siegbahn PEM, Tye JW, Hall MB. 2007 Computational studies of [NiFe] and [FeFe] hydrogenases. *Chem. Rev.* **107**, 4414–4435. (doi:10.1021/cr050185y)

59. Greco C, Bruschi M, De Gioia L, Ryde U. 2007 A QM/MM investigation of the activation and catalytic mechanism of Fe-only hydrogenases. *Inorg. Chem.* **46**, 5911–5921. (doi:10.1021/ic062320a)
60. Bruschi M, Greco C, Kaukonen M, Fantucci P, Ryde U, De Gioia L. 2009 Influence of the [2Fe]H subcluster environment on the properties of key intermediates in the catalytic cysubcluster environment on the properties of key intermediates in the catalytic cycle of [FeFe] hydrogenases: hints for the rational design of synthetic catalysts. *Angew. Chem. Int. Ed.* **48**, 3503–3506. (doi:10.1002/ange.200900494)
61. Frey M. 2002 Hydrogenases: hydrogen-activating enzymes. *ChemBioChem* **3**, 153–160. (doi:10.1002/1439-7633(20020301)3:2/3<153::AID-CBIC153>3.0.CO;2-B)
62. Volbeda A, Fontecilla-Camps JC. 2003 The active site and catalytic mechanism of NiFe hydrogenases. *Dalton Trans.* **2003**, 4030–4038. (doi:10.1039/B304316A)
63. Wait AF, Parkin A, Morley GM, dos Santos L, Armstrong FA. 2010 Characteristics of enzyme-based hydrogen fuel cells using an oxygen-tolerant hydrogenase as the anodic catalyst. *J. Phys. Chem. C* **114**, 12 003–12 009. (doi:10.1021/jp102616m)
64. Tard Cd, Pickett CJ. 2009 Structural and functional analogues of the active sites of the [Fe]-, [NiFe]-, and [FeFe]-Hydrogenases. *Chem. Rev.* **109**, 2245–2274. (doi:10.1021/cr800542q)
65. Wang M, Chen L, Sun L. 2012 Recent progress in electrochemical hydrogen production with earth-abundant metal complexes as catalysts. *Energy Environ. Sci.* **5**, 6763–6778. (doi:10.1039/c2ee03309g)
66. Du P, Eisenberg R. 2012 Catalysts made of earth-abundant elements (Co, Ni, Fe) for water splitting: recent progress and future challenges. *Energy Environ. Sci.* **5**, 6012–6021. (doi:10.1039/c2ee03250c)
67. Artero V, Chavarot-Kerlidou M, Fontecave M. 2011 Splitting water with cobalt. *Angew. Chem. Int. Ed.* **50**, 7238–7266. (doi:10.1002/anie.201007987)
68. Tran PD, Wong LH, Barber J, Loo JSC. 2012 Recent advances in hybrid photocatalysts for solar fuel production. *Energy Environ. Sci.* **5**, 5902–5918. (doi:10.1039/c2ee02849b)
69. Benson EE, Kubiak CP, Sathrum AJ, Smieja JM. 2009 Electrocatalytic and homogeneous approaches to conversion of CO_2 to liquid fuels. *Chem. Soc. Rev.* **38**, 89–99. (doi:10.1039/b804323j)
70. Fujishima A, Honda K. 1972 Electrochemical photolysis of water at a semiconductor electrode. *Nature* **238**, 37–38. (doi:10.1038/238037a0)
71. Chen X, Shen S, Guo L, Mao SS. 2010 Semiconductor-based photocatalytic hydrogen generation. *Chem. Rev.* **110**, 6503–6570. (doi:10.1021/cr1001645)
72. Kudo A, Miseki Y. 2009 Heterogeneous photocatalyst materials for water splitting. *Chem. Soc. Rev.* **38**, 253–278. (doi:10.1039/b800489g)
73. Wu M-C *et al*. 2011 Nitrogen-doped anatase nanofibers decorated with noble metal nanoparticles for photocatalytic production of hydrogen. *ACS Nano* **5**, 5025–5030. (doi:10.1021/nn201111j)
74. Tao J, Luttrell T, Batzill M. 2011 A two-dimensional phase of TiO_2 with a reduced bandgap. *Nat. Chem.* **3**, 296–300. (doi:10.1038/nchem.1006)
75. Chen X, Liu L, Yu PY, Mao SS. 2011 Increasing solar absorption for photocatalysis with black hydrogenated titanium dioxide nanocrystals. *Science* **331**, 746–750. (doi:10.1126/science.1200448)
76. Paracchino A, Laporte V, Sivula K, Grätzel M, Thimsen E. 2011 Highly active oxide photocathode for photoelectrochemical water reduction. *Nat. Mater.* **10**, 456–461. (doi:10.1038/nmat3017)
77. Tran PD, Batabyal SK, Pramana SS, Barber J, Wong LH, Loo SCJ. 2012 A cuprous oxide-reduced graphene oxide (Cu_2O–rGO) composite photocatalyst for hydrogen generation: employing rGO as an electron acceptor to enhance the photocatalytic activity and stability of Cu_2O. *Nanoscale* **4**, 3875–3878. (doi:10.1039/c2nr30881a)
78. Du A, Ng YH, Bell NJ, Zhu Z, Amal R, Smith SC. 2011 Hybrid graphene/titania nanocomposite: interface charge transfer, hole doping, and sensitization for visible light response. *J. Phys. Chem. Lett.* **2**, 894–899. (doi:10.1021/jz2002698)
79. Kay A, Cesar I, Grätzel M. 2006 New benchmark for water photooxidation by nanostructured α-Fe_2O_3 films. *J. Am. Chem. Soc.* **128**, 15 714–15 721. (doi:10.1021/ja064380l)
80. Ling Y, Wang G, Wheeler DA, Zhang JZ, Li Y. 2011 Sn-doped hematite nanostructures for photoelectrochemical water splitting. *Nano Lett.* **11**, 2119–2125. (doi:10.1021/nl200708y)
81. Xi L, Bassi PS, Chiam SY, Mak WF, Tran PD, Barber J, Loo JSC, Wong LH. 2012 Surface treatment of hematite photoanodes with zinc acetate for water oxidation. *Nanoscale* **4**, 4430–4433. (doi:10.1039/c2nr30862b)
82. Xi L, Chiam SY, Mak WF, Tran PD, Barber J, Loo SCJ, Wong LH. 2013 A novel strategy for surface treatment on hematite photoanode for efficient water oxidation. *Chem. Sci.* **4**, 164–169. (doi:10.1039/c2sc20881d)
83. Hisatomi T, Dotan H, Stefik M, Sivula K, Rothschild A, Grätzel M, Mathews N. 2012 Enhancement in the performance of ultrathin hematite photoanode for water splitting by an oxide underlayer. *Adv. Mater.* **24**, 2699–2702. (doi:10.1002/adma.201104868)
84. Gersten SW, Samuels GJ, Meyer TJ. 1982 Catalytic oxidation of water by an oxo-bridged ruthenium dimer. *J. Am. Chem. Soc.* **104**, 4029–4030. (doi:10.1021/ja00378a053)
85. Duan L, Bozoglian F, Mandal S, Stewart B, Privalov T, Llobet A, Sun L. 2012 A molecular ruthenium catalyst with water-oxidation activity comparable to that of photosystem II. *Nat. Chem.* **4**, 418–423. (doi:10.1038/nchem.1301)
86. Yamazaki H, Shouji A, Kajita M, Yagi M. 2010 Electrocatalytic and photocatalytic water oxidation to dioxygen based on metal complexes. *Coord. Chem. Rev.* **254**, 2483–2491. (doi:10.1016/j.ccr.2010.02.008)
87. Kanady JS, Tsui EY, Day MW, Agapie T. 2011 A synthetic model of the Mn_3Ca subsite of the oxygen-evolving complex in photosystem II. *Science* **333**, 733–736. (doi:10.1126/science.1206036)
88. Mukherjee S *et al*. 2012 Synthetic model of the asymmetric $[Mn_3CaO_4]$ cubane core of the oxygen-evolving complex of photosystem II. *Proc. Natl Acad. Sci. USA* **109**, 2257–2262. (doi:10.1073/pnas.1115290109)
89. Yin Q, Tan JM, Besson C, Geletii YV, Musaev DG, Kuznetsov AE, Luo Z, Hardcastle KI, Hill CL. 2010 A fast soluble carbon-free molecular water oxidation catalyst based on abundant metals. *Science* **328**, 342–345. (doi:10.1126/science.1185372)
90. Kanan MW, Nocera DG. 2008 *In situ* formation of an oxygen-evolving catalyst in neutral water containing phosphate and Co^{2+}. *Science* **321**, 1072–1075. (doi:10.1126/science.1162018)
91. Tard C *et al*. 2005 Synthesis of the H-cluster framework of iron-only hydrogenase. *Nature* **433**, 610–613. (doi:10.1038/nature03298)
92. Ogo S *et al*. 2007 A dinuclear Ni(μ-H)Ru complex derived from H_2. *Science* **316**, 585–587. (doi:10.1126/science.1138751)
93. Helm ML, Stewart MP, Bullock RM, DuBois MR, DuBois DL. 2011 A synthetic nickel electrocatalyst with a turnover frequency above 100 000 s^{-1} for H_2 production. *Science* **333**, 863–866. (doi:10.1126/science.1205864)
94. Dinca M, Surendranath Y, Nocera DG. 2010 Nickel-borate oxygen-evolving catalyst that functions under benign conditions. *Proc. Natl Acad. Sci. USA* **107**, 10 337–10 341. (doi:10.1073/pnas.1001859107)
95. Risch M, Khare V, Zaharieva I, Gerencser L, Chernev P, Dau H. 2009 Cobalt-oxo core of a water-oxidizing catalyst film. *J. Am. Chem. Soc.* **131**, 6936–6937. (doi:10.1021/ja902121f)
96. Kanan MW, Yano J, Surendranath Y, Dinca M, Yachandra VK, Nocera DG. 2010 Structure and valency of a cobalt-phosphate water oxidation catalyst determined by *in situ* X-ray spectroscopy. *J. Am. Chem. Soc.* **132**, 13 692–13 701. (doi:10.1021/ja1023767)
97. Lutterman DA, Surendranath Y, Nocera DG. 2009 A self-healing oxygen-evolving catalyst. *J. Am. Chem. Soc.* **131**, 3838–3839. (doi:10.1021/ja900023k)
98. Jiao F, Frei H. 2009 Nanostructured cobalt oxide clusters in mesoporous silica as efficient oxygen-evolving catalysts. *Angew. Chem. Int. Ed.* **48**, 1841–1844. (doi:10.1002/anie.200805534)
99. Jiao F, Frei H. 2010 Nanostructured manganese oxide clusters supported on mesoporous silica as efficient oxygen-evolving catalysts. *Chem. Commun.* **46**, 2920–2922. (doi:10.1039/b921820c)
100. Brimblecombe R, Koo A, Dismukes GC, Swiegers GF, Spiccia L. 2010 Solar driven water oxidation by a bioinspired manganese molecular catalyst. *J. Am. Chem. Soc.* **132**, 2892–2894. (doi:10.1021/ja910055a)
101. Li L, Duan L, Xu Y, Gorlov M, Hagfeldt A, Sun L. 2010 A photoelectrochemical device for visible light driven water splitting by a molecular ruthenium

catalyst assembled on dye-sensitized nanostructured TiO_2. *Chem. Commun.* **46**, 7307–7309. (doi:10.1039/c0cc01828g)

102. Li G, Sproviero EM, McNamara WR, Snoeberger RC, Crabtree RH, Brudvig GW, Batista VS. 2009 Reversible visible-light photooxidation of an oxomanganese water-oxidation catalyst covalently anchored to TiO_2 nanoparticles. *J. Phys. Chem. B* **114**, 14 214–14 222. (doi:10.1021/jp908925z)
103. Moore GF, Blakemore JD, Milot RL, Hull JF, Song H-E, Cai L, Schmuttenmaer CA, Crabtree RH, Brudvig GW. 2011 A visible light water-splitting cell with a photoanode formed by codeposition of a high-potential porphyrin and an iridium water-oxidation catalyst. *Energy Environ. Sci.* **4**, 2389–2392. (doi:10.1039/c1ee01037a)
104. Xi L *et al*. 2012 Co_3O_4-decorated hematite nanorods as an effective photoanode for solar water oxidation. *J. Phys. Chem. C* **116**, 13 884–13 889. (doi:10.1021/jp304285r)
105. Reisner E, Powell DJ, Cavazza C, Fontecilla-Camps JC, Armstrong FA. 2009 Visible light-driven H_2 production by hydrogenases attached to dye-sensitized TiO_2 nanoparticles. *J. Am. Chem. Soc.* **131**, 18 457–18 466. (doi:10.1021/ja907923r)
106. Nann T, Ibrahim SK, Woi P-M, Xu S, Ziegler J, Pickett CJ. 2010 Water splitting by visible light: a nanophotocathode for hydrogen production. *Angew. Chem. Int. Ed.* **49**, 1574–1577.
107. Tran PD, Pramana SS, Kale VS, Nguyen M, Chiam SY, Batabyal SK, Wong LH, Barber J, Loo J. 2012 Novel assembly of an MOS_2 electrocatalyst onto a silicon nanowire array electrode to construct a photocathode composed of elements abundant on the Earth for hydrogen generation. *Chem. Eur. J.* **18**, 13 994–13 999. (doi:10.1002/chem.201202214)
108. Tran PD, Artero V, Fontecave M. 2010 Water electrolysis and photoelectrolysis on electrodes engineered using biological and bio-inspired molecular systems. *Energy Environ. Sci.* **3**, 727–747. (doi:10.1039/b926749b)
109. Zhang J, Grzelczak M, Hou Y, Maeda K, Domen K, Fu X, Antonietti M, Wang X. 2012 Photocatalytic oxidation of water by polymeric carbon nitride nanohybrids made of sustainable elements. *Chem. Sci.* **3**, 443–446. (doi:10.1039/c1sc00644d)
110. Zhong DK, Cornuz M, Sivula K, Gratzel M, Gamelin DR. 2011 Photo-assisted electrodeposition of cobalt-phosphate (Co-Pi) catalyst on hematite photoanodes for solar water oxidation. *Energy Environ. Sci.* **4**, 1759–1764. (doi:10.1039/c1ee01034d)
111. Steinmiller EMP, Choi K-S. 2009 Photochemical deposition of cobalt-based oxygen evolving catalyst on a semiconductor photoanode for solar oxygen production. *Proc. Natl Acad. Sci. USA* **106**, 20 633–20 636.
112. Seabold JA, Choi K-S. 2011 Effect of a cobalt-based oxygen evolution catalyst on the stability and the selectivity of photo-oxidation reactions of a WO_3 photoanode. *Chem. Mater.* **23**, 1105–1112. (doi:10.1021/cm1019469)
113. Li L, Duan L, Wen F, Li C, Wang M, Hagfeldt A, Sun L. 2012 Visible light driven hydrogen production from a photo-active cathode based on a molecular catalyst and organic dye-sensitized p-type nanostructured NiO. *Chem. Commun.* **48**, 988–990. (doi:10.1039/c2cc16101j)
114. Lakadamyali F, Reisner E. 2011 Photocatalytic H_2 evolution from neutral water with a molecular cobalt catalyst on a dye-sensitised TiO_2 nanoparticle. *Chem. Commun.* **47**, 1695–1697. (doi:10.1039/c0cc04658b)
115. Hagfeldt A, Boschloo G, Sun L, Kloo L, Pettersson H. 2010 Dye-sensitized solar cells. *Chem. Rev.* **110**, 6595–6663. (doi:10.1021/cr900356p)
116. Tran PD, Xi L, Batabyal SK, Wong LH, Barber J, Chye Loo JS. 2012 Enhancing the photocatalytic efficiency of TiO_2 nanopowders for H_2 production by using non-noble transition metal co-catalysts. *Phys. Chem. Chem. Phys.* **14**, 11 596–11 599. (doi:10.1039/c2cp41450c)
117. Townsend TK, Browning ND, Osterloh F. 2012 Overall photocatalytic water splitting with NiO*x*–$SrTiO_3$: a revised mechanism. *Energy Environ. Sci.* **5**, 9543–9550. (doi:10.1039/c2ee22665k)
118. McKone JR, Warren EL, Bierman MJ, Boettcher SW, Brunschwig BS, Lewis NS, Gray HB. 2011 Evaluation of Pt, Ni, and Ni-Mo electrocatalysts for hydrogen evolution on crystalline Si electrodes. *Energy Environ. Sci.* **4**, 3573–3583. (doi:10.1039/c1ee01488a)
119. Hambourger M, Gervaldo M, Svedruzic D, King PW, Gust D, Ghirardi M, Moore AL, Moore TA. 2008 [FeFe]-hydrogenase-catalyzed H_2 production in a photoelectrochemical biofuel cell. *J. Am. Chem. Soc.* **130**, 2015–2022. (doi:10.1021/ja077691k)
120. Gratzel M. 2001 Photoelectrochemical cells. *Nature* **414**, 338–344. (doi:10.1038/35104607)
121. Reece SY, Hamel JA, Sung K, Jarvi TD, Esswein AJ, Pijpers JJH, Nocera DG. 2011 Wireless solar water splitting using silicon-based semiconductors and earth-abundant catalysts. *Science* **334**, 645–648. (doi:10.1126/science.1209816)
122. Rocheleau RE, Miller EL, Misra A. 1998 High-efficiency photoelectrochemical hydrogen production using multijunction amorphous silicon photoelectrodes. *Energy Fuels* **12**, 3–10. (doi:10.1021/ef9701347)
123. Jaramillo TF, Jørgensen KP, Bonde J, Nielsen JH, Horch S, Chorkendorff I. 2007 Identification of active edge sites for electrochemical H_2 evolution from MoS_2 nanocatalysts. *Science* **317**, 100–102. (doi:10.1126/science.1141483)
124. Merki D, Fierro S, Vrubel H, Hu X. 2011 Amorphous molybdenum sulfide films as catalysts for electrochemical hydrogen production in water. *Chem. Sci.* **2**, 1262–1267. (doi:10.1039/c1sc00117e)
125. Zong X, Yan H, Wu G, Ma G, Wen F, Wang L, Li C. 2008 Enhancement of photocatalytic H_2 evolution on CdS by loading MoS_2 as cocatalyst under visible light irradiation. *J. Am. Chem. Soc.* **130**, 7176–7177. (doi:10.1021/ja8007825)
126. Seger B, Laursen AB, Vesborg PCK, Pedersen T, Hansen O, Dahl S, Chorkendorff IB. 2012 Hydrogen production using a molybdenum sulfide catalyst on a titanium-protected n + p-silicon photocathode. *Angew. Chem. Int. Ed.* **51**, 9128–9131. (doi:10.1002/anie.201203585)
127. Ohno T, Bai L, Hisatomi T, Maeda K, Domen K. 2012 Photocatalytic water splitting using modified GaN:ZnO solid solution under visible light: long-time operation and regeneration of activity. *J. Am. Chem. Soc.* **134**, 8254–8259. (doi:10.1021/ja302479f)
128. Ma SK, Maeda K, Abe R, Domen K. 2012 Visible-light-driven nonsacrificial water oxidation over tungsten trioxide powder modified with two different cocatalysts. *Energy Environ. Sci.* **5**, 8390–8397. (doi:10.1039/c2ee21801a)
129. Domen K, Naito S, Soma M, Onishi T, Tamaru K. 1980 Photocatalytic decomposition of water vapour on an NiO–$SrTiO_3$ catalyst. *J. Chem. Soc. Chem. Commun.* **1980**, 543–544. (doi:10.1039/C39800000543)
130. Cobo S *et al*. 2012 A Janus cobalt-based catalytic material for electro-splitting of water. *Nat. Mater.* **11**, 802–807. (doi:10.1038/nmat3385)
131. Iwase A, Ng YH, Ishiguro Y, Kudo A, Amal R. 2011 Reduced graphene oxide as a solid-state electron mediator in Z-scheme photocatalytic water splitting under visible light. *J. Am. Chem. Soc.* **133**, 11 054–11 057. (doi:10.1021/ja203296z)
132. Abe R, Takata T, Sugihara H, Domen K. 2005 Photocatalytic overall water splitting under visible light by TaON and WO_3 with an IO_3^-/I^- shuttle redox mediator. *Chem. Commun.* 3829–3831. (doi:10.1039/b505646b)
133. Maeda K, Abe R, Domen K. 2011 Role and function of ruthenium species as promoters with TaON-based photocatalysts for oxygen evolution in two-step water splitting under visible light. *J. Phys. Chem. C* **115**, 3057–3064. (doi:10.1021/jp110025x)
134. Higashi M, Abe R, Takata T, Domen K. 2009 Photocatalytic overall water splitting under visible light using $ATaO_2N$ (A = Ca, Sr, Ba) and WO_3 in a IO_3^-/I^- shuttle redox mediated system. *Chem. Mater.* **21**, 1543–1549. (doi:10.1021/cm803145n)
135. Le Goff A, Artero V, Jousselme B, Tran PD, Guillet N, Metaye R, Fihri A, Palacin S, Fontecave M. 2009 From hydrogenases to noble metal-free catalytic nanomaterials for H-2 production and uptake. *Science* **326**, 1384–1387. (doi:10.1126/science.1179773)
136. Tran PD *et al*. 2012 Copper molybdenum sulfide: a new efficient electrocatalyst for hydrogen production from water. *Energy Environ. Sci.* **5**, 8912–8916. (doi:10.1039/c2ee22611a)